

# A Comparative Study of Aerial Photographs and LIDAR Imagery for Landslide Detection in the Puget Lowland, Washington

by Ryan D. Gold

WASHINGTON  
DIVISION OF GEOLOGY  
AND EARTH RESOURCES  
Open File Report 2004-6  
February 2004



WASHINGTON STATE DEPARTMENT OF  
**Natural Resources**  
Doug Sutherland - Commissioner of Public Lands



# **A Comparative Study of Aerial Photographs and LIDAR Imagery for Landslide Detection in the Puget Lowland, Washington**

---

by Ryan D. Gold

WASHINGTON  
DIVISION OF GEOLOGY  
AND EARTH RESOURCES  
Open File Report 2004-6  
February 2004



WASHINGTON STATE DEPARTMENT OF  
**Natural Resources**  
Doug Sutherland - Commissioner of Public Lands

**DISCLAIMER**

Neither the State of Washington, nor any agency thereof, nor any of their employees, makes any warranty, express or implied, or assumes any legal liability or responsibility for the accuracy, completeness, or usefulness of any information, apparatus, product, or process disclosed, or represents that its use would not infringe privately owned rights. Reference herein to any specific commercial product, process, or service by trade name, trademark, manufacturer, or otherwise, does not necessarily constitute or imply its endorsement, recommendation, or favoring by the State of Washington or any agency thereof. The views and opinions of authors expressed herein do not necessarily state or reflect those of the State of Washington or any agency thereof.

**WASHINGTON DEPARTMENT OF NATURAL RESOURCES**

Doug Sutherland—*Commissioner of Public Lands*

**DIVISION OF GEOLOGY AND EARTH RESOURCES**

Ron Teissere—*State Geologist*

David K. Norman—*Assistant State Geologist*

Washington Department of Natural Resources  
Division of Geology and Earth Resources  
PO Box 47007  
Olympia, WA 98504-7007  
*Phone:* 360-902-1450  
*Fax:* 360-902-1785  
*E-mail:* [geology@wadnr.gov](mailto:geology@wadnr.gov)  
*Website:* <http://www.dnr.wa.gov/geology/>

## PREFACE

The Washington Division of Geology and Earth Resources is proud to publish, in open-file format, the undergraduate thesis of Ryan D. Gold—*A Comparative Study of Aerial Photographs and LIDAR Imagery for Landslide Detection in the Puget Lowland, Washington*. This publication consists of three components: (1) the thesis text, (2) a detailed landslide inventory and geologic map of the study area, and (3) geographic information systems (GIS) files (in ESRI shapefile format) and metadata for inventory landslides, landslide scarps, and surficial geology.

This study, conducted during the summer of 2002, evaluates the effectiveness of aerial photograph and LIDAR (Light Detection and Ranging) remote sensing techniques in an effort to determine which method is the most efficient, accurate, and precise for identifying landslides and landslide hazard areas in western Washington. For this research, five miles of coastline in southeastern Kitsap County, Washington was selected based upon LIDAR availability, geologic setting, and property ownership constraints. This study area stretches along the eastern shore of Hood Canal from the Kitsap–Mason County line in the south to Hood Point in the north. Independent landslide inventories were developed from each remote sensing dataset, and approximately half of the identified landslides were subsequently verified through field observations. The resulting landslide inventory should be of benefit to land managers, civic planners, and the general public.

We present this thesis as academic research that was conducted, in part, with personnel and financial support from the Washington State Department of Natural Resources. Gold received financial support in the form of a grant from Whitman College, through the Whitman College Parents' Council. The Puget Sound LIDAR Consortium also provided technical support. With the exception of a very few corrections to spelling and wording, the thesis text and map are presented here exactly as submitted to Whitman College.

The Washington State Department of Natural Resources is keenly interested in emerging technologies that may be applied to the identification and mitigation of potential geologic hazards, including landslide hazards. The ability to map large areas for landscape features, such as landslides, in an efficient and accurate manner is critical to land management agencies, municipal and county governments, and geotechnical consultants. Identification of landslides and landslide hazard areas via the use of LIDAR technologies may improve upon previous methods.

KARL W. WEGMANN  
STEPHEN P. PALMER



A COMPARATIVE STUDY OF AERIAL PHOTOGRAPHS AND LIDAR IMAGERY  
FOR LANDSLIDE DETECTION IN THE PUGET LOWLAND, WASHINGTON

by

Ryan D. Gold

A thesis submitted in partial fulfillment  
For graduation with Honors in Geology

Whitman College  
2003

## Certificate of Approval

This is to certify that the accompanying thesis by Ryan D. Gold has been accepted in partial fulfillment of the requirements for graduation with Honors in Geology

---

Patrick Spencer

---

Robert Carson

Whitman College  
2003



## TABLE OF CONTENTS

|   |     |
|---|-----|
| Title Page.....                                 | i   |
| Certificate of Approval.....                    | ii  |
| Table of Contents.....                          | iii |
| List of Illustration.....                       | iv  |
| <br>  |     |
| Abstract.....                                   | 1   |
| Introduction.....                               | 2   |
| Project History.....                            | 6   |
| Location and Geologic Setting.....              | 8   |
| Location.....                                   | 8   |
| Previous Work.....                              | 8   |
| Glacial History.....                            | 9   |
| Geology and Stratigraphy.....                   | 10  |
| Climate.....                                    | 13  |
| Vegetation.....                                 | 13  |
| Landslides.....                                 | 15  |
| Landslide Classification.....                   | 16  |
| Landslide Morphology.....                       | 19  |
| Landslide Causes.....                           | 20  |
| Stages in Landslide Evolution.....              | 21  |
| Landslide Mitigation.....                       | 22  |
| Methods.....                                    | 23  |
| Aerial Photographs.....                         | 23  |
| LIDAR Imagery.....                              | 25  |
| Digitization.....                               | 31  |
| Field Methods .....                             | 34  |
| Data and Results.....                           | 37  |
| Discussion.....                                 | 40  |
| Comparison of Aerial Photographs and LIDAR..... | 40  |
| Characterization of Sliding in Study Area.....  | 57  |
| Landslide Inventory.....                        | 59  |
| Conclusion.....                                 | 60  |
| Acknowledgements.....                           | 62  |
| Appendix.....                                   | 63  |
| Landslide Inventory Data.....                   | 63  |
| Works Cited.....                                | 65  |

## LIST OF ILLUSTRATIONS

### Figures

|  |    |
|--|----|
| Figure 1a,b: (a) Map of study area in Washington and (b) study area with types of landsliding indicated.....     | 3  |
| Figure 2: Example of LIDAR & aerial photo imagery.....   | 4  |
| Figure 3: Map of ice extent from Vashon glaciation.....  | 9  |
| Figure 4: Idealized stratigraphic columns for study area.....  | 11 |
| Figure 5: Average rainfall per year map.....   | 14 |
| Figure 6: Schematic of shallow and deep-seated landslides.....   | 17 |
| Figure 7: Shallow landslide and pistol-butt trees.....   | 17 |
| Figure 8: Deep-seated landslide and bowing trees.....  | 18 |
| Figure 9: Landslide morphology nomenclature.....   | 19 |
| Figure 10: Orthophotograph and LIDAR image showing field are divided into two sections.....                      | 23 |
| Figure 11: Aerial photograph acquisition.....  | 24 |
| Figure 12: Stereoscope.....  | 25 |
| Figure 13: LIDAR acquisition.....  | 26 |
| Figure 14a-f: Different sun positions for LIDAR imagery .....  | 30 |
| Figure 15: LIDAR showing landslide morphology.....   | 31 |
| Figure 16: Digitization process with polygons representing the body of slides and lines for scarp headwalls..... | 32 |
| Figure 17: Deep seated slide with aerial photograph pair and LIDAR image.....                                    | 41 |
| Figure 18a-e: Anderson creek slide, showing better precision with LIDAR.....                                     | 44 |
| Figure 19: Scarp within poorly defined slide boundary.....   | 45 |
| Figure 20a-c: Debris on beach comparison—(a) on airphoto, (b) LIDAR, (c) from the ground.....                    | 47 |
| Figure 21b: Examples of usefulness of vegetation penetrating LIDAR (a) esker, (b) trellis drainage.....          | 48 |
| Figure 22-e: Poor resolution of LIDAR.....   | 50 |
| Figure 23 LIDAR availability.....  | 56 |

### Tables

|  |    |
|--|----|
| Table 1: Aerial photograph success.....                                  | 37 |
| Table 2: LIDAR imagery success.....                                      | 37 |
| Table 3: Real slides.....  | 38 |
| Table 4: Comparison of imagery for locating deep and shallow slides..... | 38 |
| Table 5: Slide type and location.....                                    | 39 |

### Plates

|   |  |
|---|--|
| Plate 1: Geology of field area with LIDAR & topographic map as background |  |
|---|--|

TITLE: A comparative study of aerial photographs and LIDAR imagery for landslide detection in the Puget Sound, Washington.

## ABSTRACT

Landslides in western Washington cause millions of dollars in damage each year. Accurate and precise remote sensing techniques are a necessary first step in creating useful landslide inventories for future land use planning and engineering mitigation decisions. Both aerial photos and LIDAR (Light Distance and Ranging) imagery were evaluated and compared on the basis of the accuracy of landslide location and the precision of landslide boundary definition for an eight-kilometer stretch of heavily forested coast along Hood Canal, Kitsap County, Washington, an area which is characterized by numerous slides occurring in Pleistocene glacial and non-glacial sediments. Independent landslide inventories were developed from each remote sensing dataset and were followed by field observations of approximately half of the identified slides.

A geologic map and complete landslide inventory for the eight-kilometer stretch of coast was created. In the southern reaches of the field area, a thick unit of pre-Vashon gravel (Qpg.) comprises the basal unit, overlain by Vashon advance outwash (Qgas), in turn overlain by Vashon till (Qgt) which mantles the upper plateau throughout the field area. Landsliding in this area is characterized by shallow, colluvial slides. In the northern reaches of the field area, non-glacial sediments including stratified silts and clays comprise the basal unit which is overlain by advance outwash and till from the Vashon Stade. The non-glacial sediments act as an aquatard, increasing pore-water pressures in the sediments above, and resulting in large-scale, deep-seated landslides.

Results suggest that the two methods yield similar results for the identification of slides. However, other factors such as the type of sliding, precision of slide boundary definition, vegetation, cost, imagery availability, and user efficiency show varied results. Photogrammetry is effective for locating small, shallow slides occurring along coastal bluffs as well as larger, deep-seated slides, costs only \$25/mi<sup>2</sup> to fly, works well when vegetation cues indicate recent sliding, and is available throughout Washington State in multi-year intervals. LIDAR imagery is highly effective for precisely defining landslide boundaries where the laser return from the ground is good, is efficient in the field and office, is easier to interpret than aerial photographs, and is highly manipulatable with respect to shadows and vertical exaggeration. Results from this comparison suggest that both methods have strengths and weaknesses with regard to generating landslide inventories and that the best approach is to use both methods in a complementary fashion.

## INTRODUCTION

During the winter of 1996-1997, intense rainfall triggered shallow, fast moving landslides throughout the central Puget Lowland, causing tens of millions of dollars in damage and six deaths (Shipman, 2001). Just two years later, during the 1998-1999 winter, prolonged heavy rainfall reactivated dormant, deep-seated landslides, forcing nearly a hundred families to abandon their homes, and again causing millions of dollars in damage (Shipman, 2001). Clearly, landslides in the Puget Lowland pose a serious geologic hazard. A study commissioned by the Federal Emergency Management Agency and carried out by the Washington State Department of Ecology states that a vital step for improving Washington State's management of landslide hazards is "improved identification and mapping of landslide hazards, making use of good quality geologic information, high-resolution topographic mapping, and systematic inventories of both past and future landslide activity" (Shipman, 2001, p. xi).

This study, conducted during the summer of 2002, evaluates two remote sensing techniques in an effort to determine which method allows professionals dealing with landslide hazards to most efficiently, accurately, and precisely identify landslides. A detailed geologic map and complete landslide inventory for an eight kilometer stretch of coast along Hood Canal in eastern Kitsap County is also presented (Figure 1a & b).

Accurate and precise remote sensing techniques are a necessary first step in creating useful landslide inventories for future land use planning and engineering mitigation decisions because areas where past landsliding has occurred are potential sites of future landsliding. Aerial photographs have been a standard in the remote sensing field for many years (Figure 2), but newer technologies purport to offer even more

**Figure 1a:**  
Hood Canal  
with study area  
indicated  
(modified from  
mapquest.com,  
2003).

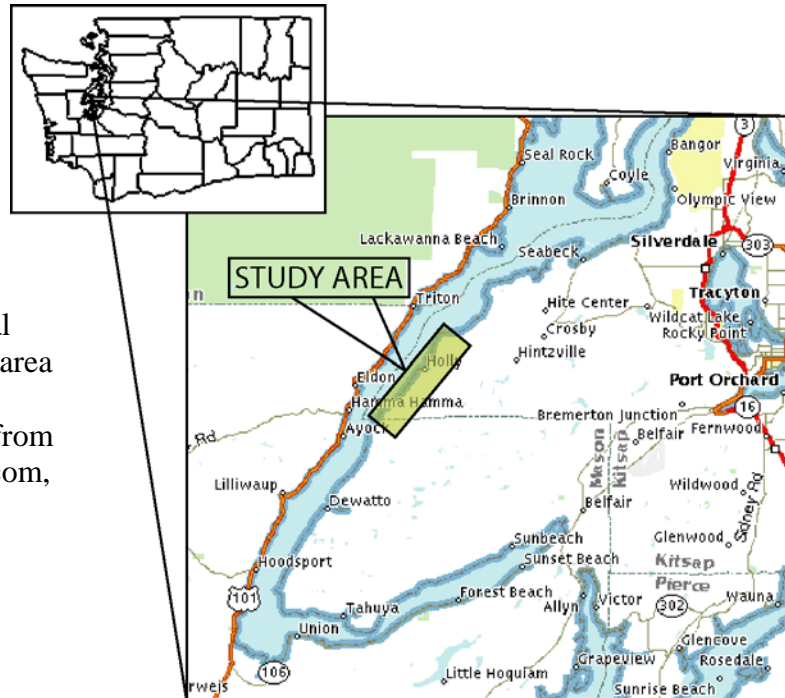
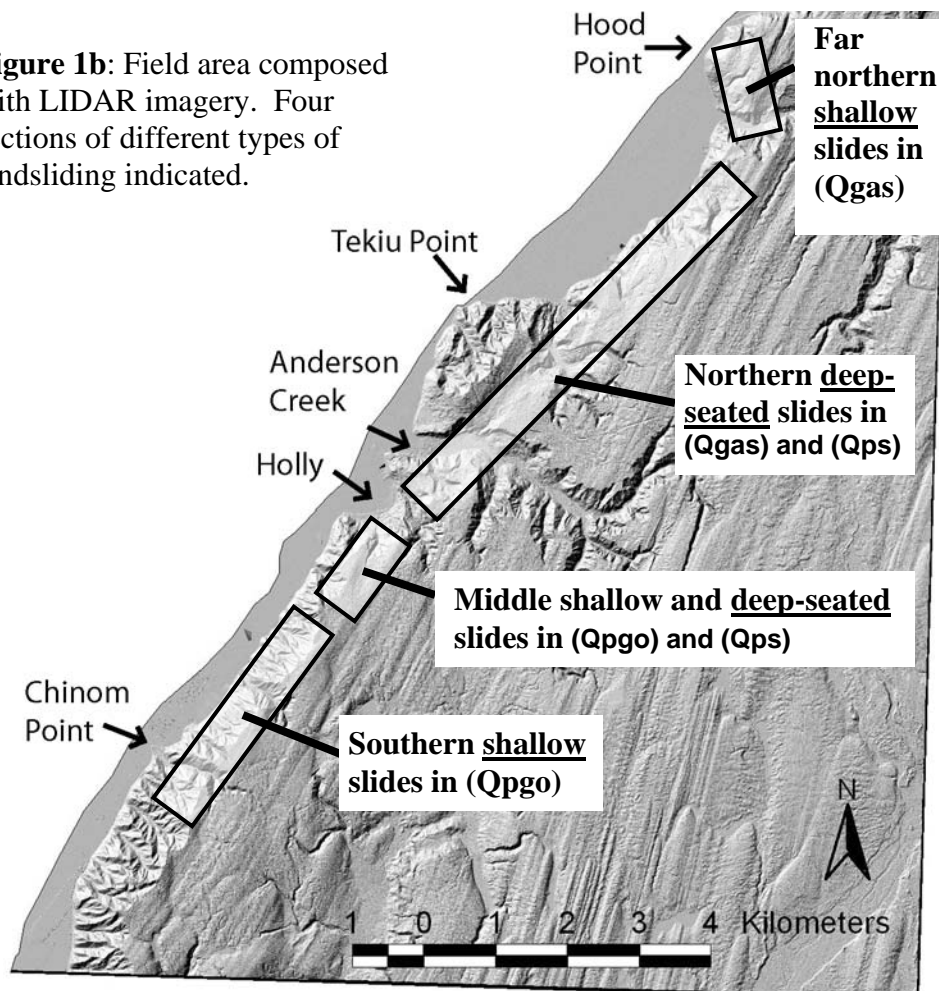


**Figure 1b:** Field area composed  
with LIDAR imagery. Four  
sections of different types of  
landsliding indicated.



detailed, accurate, and easy to interpret images of the earth's surface. A new technology, LIDAR (LIght Distance and Ranging), was recently used to conduct a survey of the Puget Lowland, including Kitsap County. LIDAR employs a laser, which shoots thousands of pulses per second at the ground surface via a multi-faceted rotating mirror deployed from a low-flying aircraft. The resulting high resolution LIDAR dataset of elevation points for the land surface can then be "processed" via a series of algorithms to eliminate signals from vegetation (Haugerud and Harding, 2001). The final product is a digital, "virtually deforested" image of the bare earth surface (Figure 2).

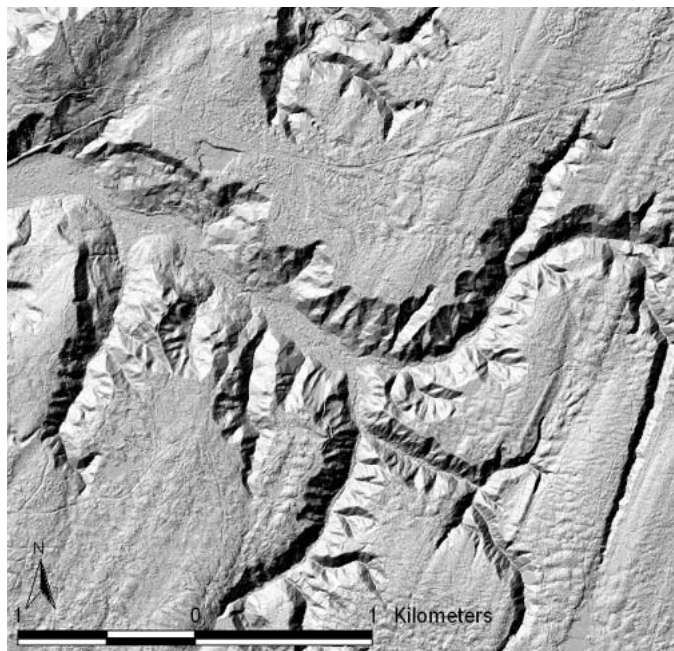
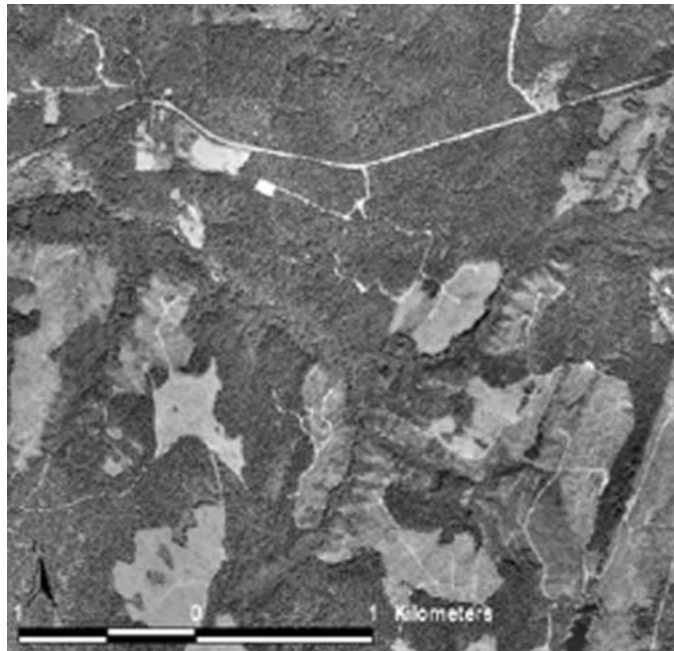


**Figure 2:** A comparison of an aerial photograph (top) to LIDAR imagery (bottom).

Both aerial photographs and LIDAR imagery were evaluated and compared on the basis of the accuracy of landslide location and the precision of landslide boundary definition for an eight kilometer stretch of heavily forested coast along Hood Canal, Kitsap County, Washington. The stretch of coastline chosen for the study is characterized by numerous slides occurring in Pleistocene glacial and non-glacial sediments. Independent landslide inventories were developed from each remote sensing dataset and were followed by field observations during which approximately half of the identified slides were visited.

In addition to comparing aerial photographs and LIDAR imagery, a geologic map and complete landslide inventory for the study area was created. In the southern portion of the field area, a 100m thick unit of pre-Vashon gravel (Qpg<sub>o</sub>) comprises the basal unit. This is overlain by advance outwash from the Vashon Stade (Qgas), which is blanketed by the Vashon till (Qgt) which mantles the upper plateau throughout the field area. Landsliding in this area is characterized by shallow, colluvial slides. In the northern portion of the field area, non-glacial sediments (Qps), including stratified silts and clays, comprise the basal unit which is overlain by advance outwash (Qgas) and till (Qgt) from the Vashon Stade. The predominantly fine-grained non-glacial sediments act as an aquatard, increasing pore water pressures in the overlying sediments. This appears to be a driving force in causing large-scale deep-seated landslides within the study area (Figure 1b).

It is my hope that results from this study can be used to efficiently create accurate and precise landslide inventories for the Puget Lowland and perhaps in other landslide-

prone regions throughout the world. Hopefully, inventories such as these, as well as detailed geologic maps, can be used to mitigate future landslide threats.

## **Project History**

During my junior year at Whitman College, in search of a potential thesis topic, I contacted Whitman College alumnus Karl Wegmann and his colleague, Steve Palmer. They are both geologists with the Washington State Department of Natural Resources' (DNR) Division of Geology and Earth Resources (DGER). We collaborated to design a project in which conventional aerial photographs would be compared and imagery produced from LIDAR for landslide detection. The location of the study area was constrained by the availability of LIDAR data and property ownership. A stretch of coastline along the eastern shore of Hood Canal, Washington in the Puget Lowland was selected. Robert Carson, a faculty advisor, mapped the coastal bluffs just south of this area from 1972 to 1974. Having identified an appropriate study area, permission was obtained from the landowners in the area to conduct field verification of the landslides. The Puget Sound LIDAR Consortium (PSLC), the agency that provided the necessary data to create the desired imagery, was also contacted.

Ten weeks were spent at the DGER office in Olympia, Washington. The first week was spent acquiring the aerial photographs covering the study area and becoming acquainted with the geology of the Puget Lowland. During that week, Wegmann also led a field trip to some well-known landslides in the Olympia area. Weeks two through four were spent learning and applying the techniques of photogrammetry to create a landslide inventory for the southern two-thirds of the field area. The fifth week was spent



becoming acquainted with the ESRI GIS software programs ArcView and ArcInfo as well as creating hillshaded imagery from LIDAR data covering my field area. During the sixth week, a landslide inventory was created for the entire field area from LIDAR imagery. The remaining time was spent between the DGER office refining the digital aspects of the project and in the field, mapping the local geology and field-verifying landslides.

Throughout the fall, contact was maintained with Wegmann and Palmer. In early January, another week was spent in Olympia, further refining figures and data for the project as well as making a final field-reconnaissance survey of coastal slopes when leaf cover was at a minimum.

## LOCATION AND GEOLOGIC SETTING

### **Location**

The study area is on the western shore of the Kitsap Peninsula, which is bounded by Hood Canal to the west and Puget Lowland to the east (Figure 1a & b). The Puget Lowland is bordered by the Cascade Mountains on the east and the Olympic Mountains on the west (Deeter, 1979). The Olympic Mountains contain approximately 12,000 km<sup>2</sup> of rugged, glaciated peaks. The mountains are geologically young, having experienced uplift since the mid-Tertiary (Brandon et al., 1998).

### **Previous Work**

Many geologists have studied the area, with the most thorough and complete works conducted by Jerald Deeter (1979) and Jeffrey Gryta (1975). Deeter's master's thesis, entitled "Quaternary Geology and Stratigraphy of Kitsap County, Washington" (1979) offers a detailed geologic map as well as useful descriptions of Pleistocene units. Gryta's master's thesis, entitled "Landslides along the western shore of Hood Canal, northern Mason County, Washington" (1975) characterizes landsliding that occurs south and directly across Hood Canal from my study area. The area is also included in the *Coastal Zone Atlas of Washington* (Washington Department of Ecology, 1979). The maps produced in this volume were created from Deeter's thesis work. No previous detailed landslide inventory maps exist for the study area. In addition to comparing remote sensing techniques, a goal of this study is to produce a detailed landslide inventory for the area.

## Glacial History

The shoreline along Hood Canal is composed of Pleistocene glacial and interglacial sediments (Shipman, 2001). In general, north-south trending ridges characterize the glacial drift plain of the upland of the area. These ridges are typically mantled by glacial till that is underlain by older glacial and interglacial deposits, while the valleys contain glacial outwash and recent alluvium (Deeter, 1979). Aside from a few exposures of Tertiary igneous and sedimentary rocks, the outcrops in Kitsap County are Pleistocene in age (Deeter, 1979). These Pleistocene sediments have been deposited over the course of a series of glacial events from 1,000,000 years ago to the present. Units will be referred to as either pre-Vashon (penultimate glacial event) or Vashon (most recent glacial event). An ice lobe passed over Kitsap Peninsula 15,900 years ago when the Vashon Stade reached its maximum (Porter and Swanson, 1998) (Figure 3).

**Figure 3:** Extent of glaciation during the Vashon Stade (University of Washington, 2003)



## Geology and Stratigraphy

The abundance of complex glacial and non-glacial sediments and landforms that exist in the Puget Lowland is astounding. There are deltas, moraines, advance and recessional outwash, lodgement and ablation till, glacio-lacustrine deposits, a variety of interglacial deposits, and eolian sediments. Distinguishing these deposits to construct an accurate glacial history for the Puget Lowland is a difficult and labor-intensive task, which is further complicated by differing opinions on the ages, names, and overall glacial history of the Puget Lowland. For the sake of simplicity, as well as relevance to this project, Jerald Deeter's nomenclature and depositional history will be used. This study will focus on the physical characteristics of the glacial and interglacial units because factors like permeability and cohesive strength aid in understanding stratigraphic control on landsliding along Hood Canal (Figure 4).

### *Interglacial beds (Qps)*

The lowermost and oldest stratigraphic unit is a highly compact, stratified, gray, clayey silty-sandy unit with dark pieces of compressed, peaty wood (Qps). This unit acts as an aquatard. It is interpreted to have been deposited during a non-glacial interval prior to Fraser Glaciation. This unit appears in the study area just south of Holly and is almost continuous to just south of Hood Point (Figure 4, Plate 1).

### *Pre-Vashon gravels (Qpg<sub>o</sub>)*

Overlying the interglacial unit is an over-consolidated, impermeable, oxidized pebble-to-cobble gravel. The unit exhibits poor bedding and its clasts are primarily composed of basalt, slate, and sandstone; Deeter (1979) mapped this unit as Skokomish Gravels and interpreted it to represent outwash from the Olympic Mountains. For this

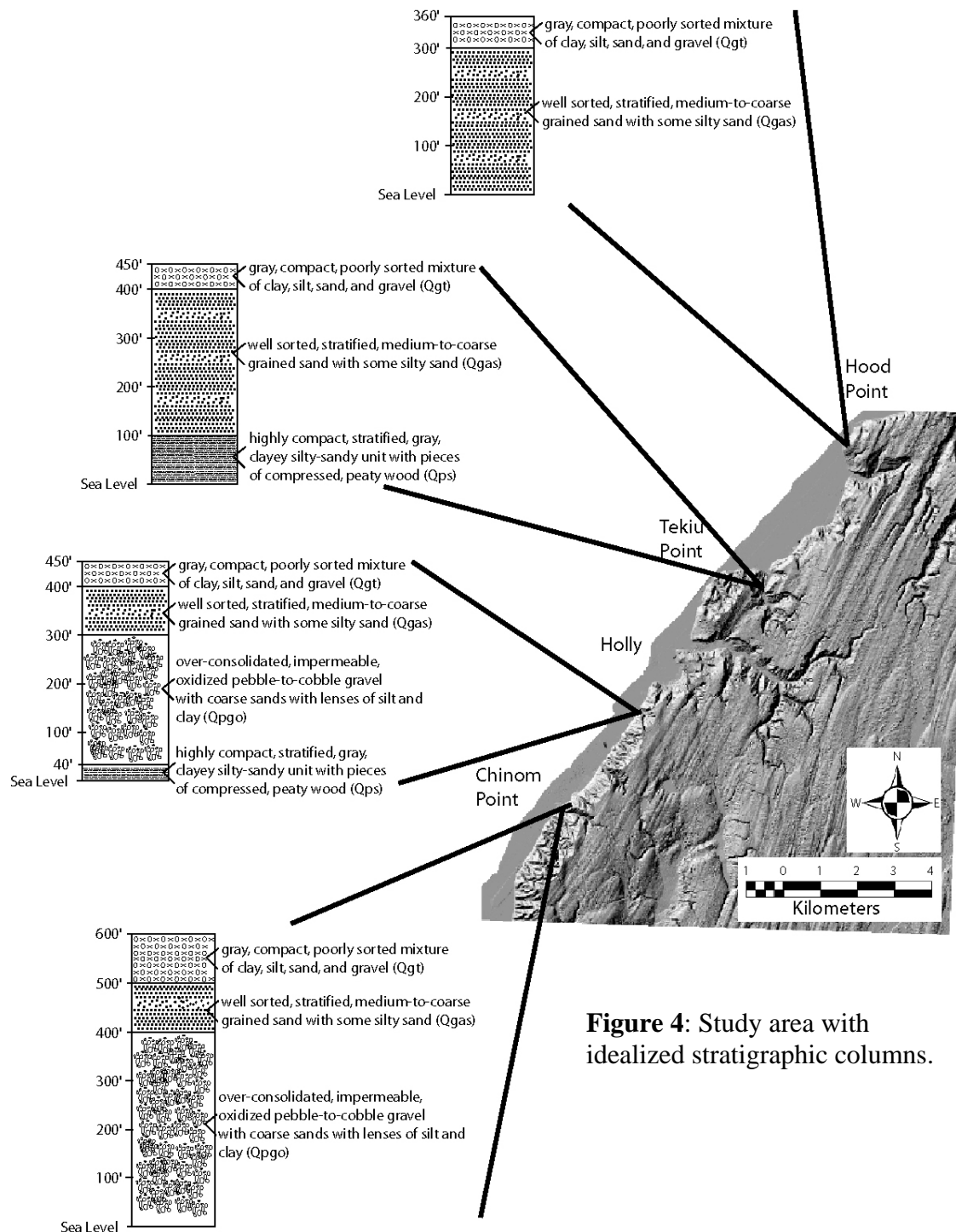


**Figure 4:** Study area with idealized stratigraphic columns.

study, it will be referred to as the pre-Vashon gravels (Qpgo). In the southern portion of my field area, the gravel is roughly 100-meters thick and it gradually pinches out to the north, disappearing entirely near the town of Holly (Figure 4, Plate 1).

*Vashon advance outwash (Qgas)*

A prevalent unit within the study area is outwash deposits from the advancing Puget lobe of the Cordilleran ice sheet. As the glacial lobe neared the study area, sandy, braided streams abounded and the resulting deposits grade from fine-to medium-grained sand in the lower portions of the unit to coarse-grained sand with lenses of gravel in the upper portion of the unit (Qgas). This highly permeable unit is found throughout the study area, and averages roughly 30 meters in thickness (Figure 4, Plate 1).

*Vashon till (Qgt)*

In the upland portions of the study area, poorly sorted clay, silt, sand, and gravel mantle the topography (Qgt) (Figure 4, Plate 1). This unit is till from the Vashon Stade when ice advanced over the land approximately 15,900-14,000 years ago (Borden et al., 2001). Till was deposited during the advance and retreat of the Vashon ice.

*Vashon recessional outwash (Qgo)*

Recessional outwash from the retreat of the Vashon ice varies greatly in extent and thickness. It is stratigraphically above the Vashon till. It is poorly sorted compared to the advance outwash, consisting of fine-to coarse-grained sand with some gravel. It ranges in thickness from 0.5 to 3 meters and is found sporadically in the upland area (Deeter, 1979). For mapping purposes Qgo is combined with Qgt in the upland surfaces, except where the thickness of Qgo warranted separate delineation (Figure 4, Plate 1). This is reasonable because of the intermittent deposition of Qgo on top of Qgt and because the field work focused primarily on the bluffs where landsliding occurs.

### *Holocene alluvium, peat, and landslide deposits (Qa, Qb, Qp, Qls)*

Since the last glacial event, unconsolidated clays, silts, sands, and gravels have accumulated in stream valleys (Qa), along beaches (Qb) via fluvial, near-shore marine and mass-movement processes, and in upland pond and marsh settings (Qp). In addition, a thin layer of soil and colluvium has formed and now mantles much of the field area. Also, landslide deposits (Qls) cover many of the steep, unstable slopes in the study area (Figure, Plate 1).

### **Climate**

In his discussion of the climate of Hood Canal, Gryta (1975) indicates that the area is characterized by bi-modal prevailing wind directions and high barometric pressures in the summer and low barometric pressures in the winter characterize the area. The late spring and summer months are dominated by westerly winds that circulate clockwise around high-pressure systems and bring dry, cool air to the area. In the late fall and winter, westerly and southwesterly winds, influenced by counter-clockwise rotation around low-pressure systems, bring warm, moist air into the area. The result of this bi-modal climate pattern is that the majority of the area's annual precipitation, 152-centimeters per year, is concentrated in the winter months (Figure 5).

### **Vegetation**

The western shore of the Kitsap Peninsula is heavily vegetated, which leads to difficulties with remote sensing techniques. The upper canopy is dominated by

deciduous and coniferous trees including Douglas-Fir, western red cedar, western hemlock, and madrona. The lower canopy and ground cover is dominated by smaller

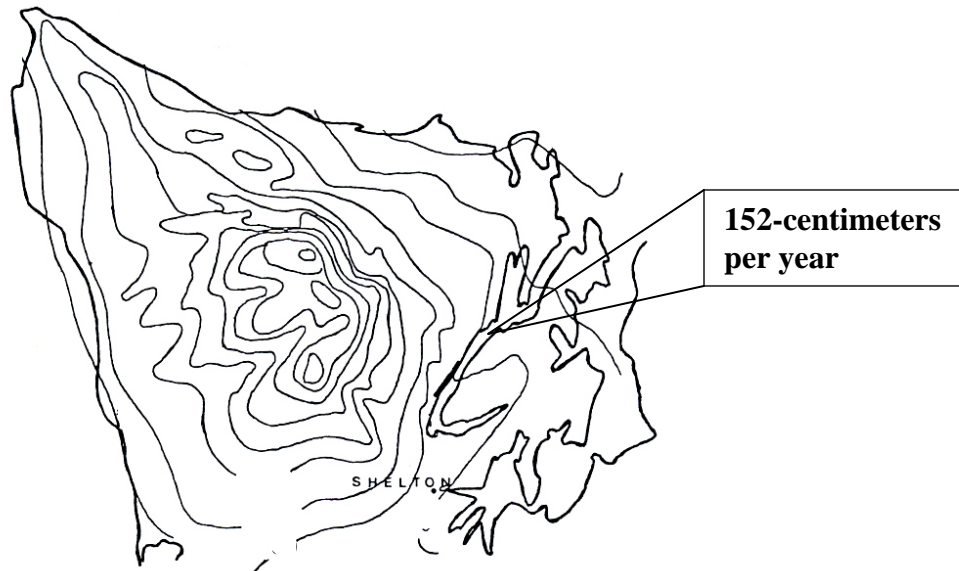


**Figure 5:** Average rainfall per year in northwestern Washington (modified from Gryta, 1975).

trees and shrubs including red alder, big-leaf and vine maple, evergreen huckleberry, scotch broom, salal, oregon grape, rhododendron, blackberry, devilsclub, a variety of ferns, and horsetail.



## LANDSLIDES

Landsliding is a general term covering a wide variety of mass-movement processes involving the downslope transport, under gravitational influence, of soil and rock material en masse. Usually the displaced material moves over a relatively confined zone or surface of shear (Jackson, 1997). Gravity is the driving force facilitated by increased precipitation, undercutting of the slope via erosion, as well as through the physical characteristics (weaknesses) of certain stratigraphic layers. According to the USGS:

“landslides, including debris flows, are a national problem. They occur in significant numbers in all 50 states and are widespread in the U.S. island territories. Landslides disrupt communities and lifelines, transportation corridors, fuel and energy conduits, and communication linkages. It is estimated that landslide-related fatalities average from 25 to 50 per year, and that direct and indirect economic costs to the nation range up to \$2 billion per year” (Geologic Hazards, 1998).

The Puget Lowland of Washington is no exception, with landslides affecting approximately 1000-kilometers of the Puget Sound’s shoreline, “reflecting the pervasiveness of high, steep coastal bluffs and the widespread occurrence of geologic conditions that can give rise to slope failures” (Shipman, 2001, p. x).

Gryta (1975) characterizes landslides across Hood Canal from this study area. He summarizes that large slump earthflows “occurred soon after the final Pleistocene deglaciation...activated when the ice support of valley slope materials was reduced with melting of the...glaciers” (p. i). Since the retreat of ice, landslides have continued to affect the area. He states that the activation of landslides that have resulted since the loss of ice support for valley slopes is “directly related to rainfall, and localized stratigraphic and/or slope conditions” (p. i).

Gryta also concludes that large, deep-seated slides occur on 30-45% of slopes and that they occur in the winter months, when rainfall exceeds average annual precipitation by more than 30-centimeters, in situations where permeable layers overlie impermeable layers. He further asserts that shallow slides occur on 35-60% of slopes and that they can occur at any time during the year when triggered by intense rainfall and that they displace surficial sand, gravel, and soil but not the underlying somewhat consolidated geologic units.

### **Landslide Classification**

The classification system for landslides is complex and varied. For the purposes of this study, terminology is adapted from Shipman (2001) and summarized from Cruden and Varnes (1996). There are a variety of landslides occurring in this study area, and while they could be endlessly subdivided, two distinctions are particularly important and descriptive:

1. Shallow landslides are defined as slides that have a depth of failure within the soil and/or colluvial mantle, and generally are smaller than deep-seated landslides (Gerstel, 1997) (Figure 6). Areas of steep topography may be at higher risk for shallow landsliding as a result of a thinner soil and colluvial layer in these steeper areas. Shallow landslides often initiate on the main scarp of large deep-seated landslides, or where rotational blocks of the larger deep-seated slide have resulted in over-steepening of segments of the slope, where drainages have been disrupted and redirected, and where material strengths have been reduced (Gerstel, 1999). These slides are often very localized and small (Figure 7). Also, shallow landsliding may occur on slopes where

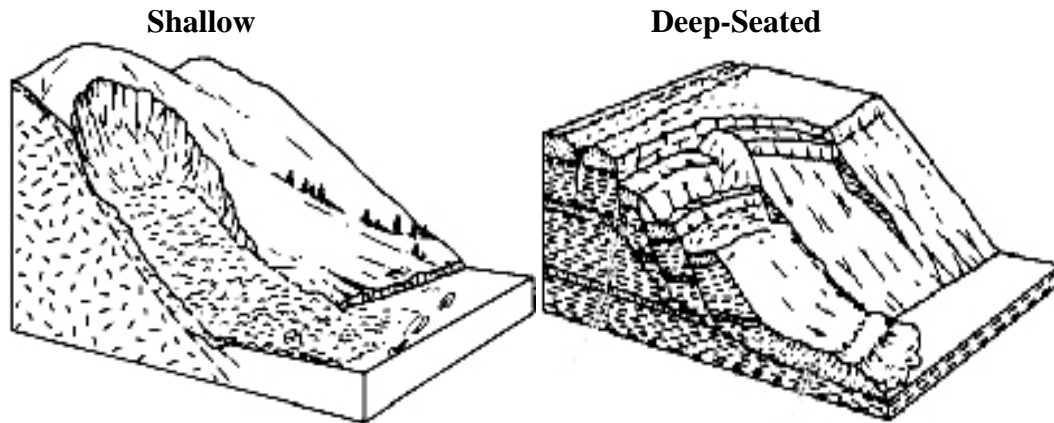


**Figure 6:** Shallow landslide (left) compared to deep-seated landslide (right). Notice that failure surface of shallow landslide does not penetrate consolidated sediments, whereas the failure surface of the deep-seated landslide penetrates into the consolidated sediments.



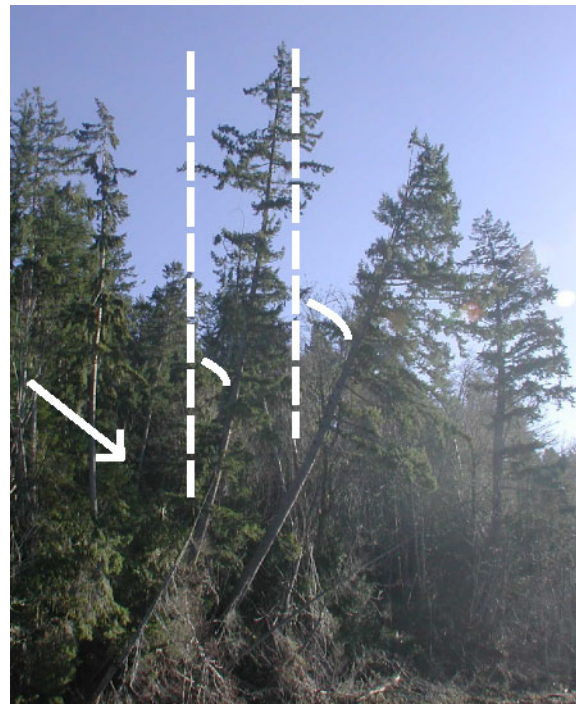
**Figure 7:** Shallow slide north of Tekiu Point (left) and pistol-butt trees on south shore of Anderson Cove indicating colluvial creep (right).

there is extensive creep, as exhibited by pistol butt trees (Figure 7), especially during periods of higher than average precipitation.

2. Deep-seated landslides are defined as slides that fail below the rooting depth of the vegetation and generally into the bedrock or sediments below the soil or colluvial layer (Figures 6 & 8), and are often large in aerial extent. These landslides are activated and often reactivated by either natural causes or land management practices. They often prove difficult or impossible to mitigate from a cost-benefit perspective. Cruden and Varnes (1996) classify deep-seated landslides based upon their mechanism of movement into falls, topples, slides, and flows. Deep-seated landslides occur in bedrock as well as coarse (debris) and fine (earth) soils and are difficult to model analytically. As a result, identification of existing landslides serves as one of the best indicators of the potential for future landslides (Gerstel, 1997). Trees, particularly evergreens, growing on active or intermittently active deep-seated landslides often exhibit a “bow” shape (Figure 8).



**Figure 8:** Deep-seated slide in Seattle, WA (above) (WDGER photos). Bowing trees that indicate deep-seated slide movement south of Holly (right).



Slides in the study area were also classified based on the state of their activity. Slides were described as (1) *active*, implying that a slide moved in the last annual cycle

of seasons; (2) *young*, implying that a slide is stable at present, but appears prone to sliding in the near future; or (3) *dormant*, implying that the slide has been stable for more than ten years, though may be reactivated during extremely intense and prolonged periods of precipitation.

## Landslide Morphology

Nomenclature important to describing landslide morphology is illustrated in Figure 9, adapted from Cruden and Varnes (1996). Several features were important to

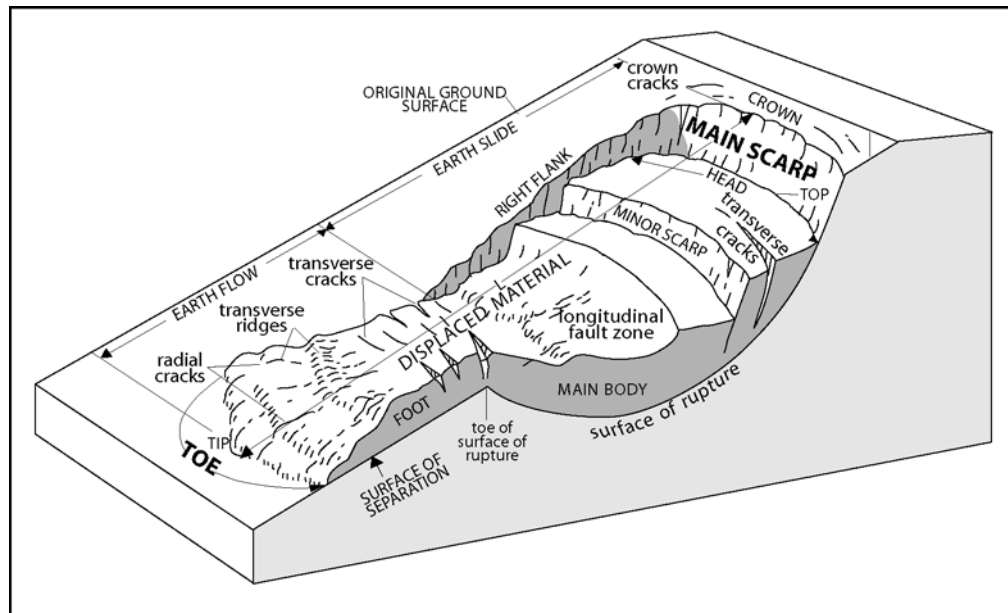


**Figure 9:** Landslide morphology with key features (scarp and toe) indicated in bold (modified from Varnes (1978) and Cruden and Varnes (1996)).

landslide location on both aerial photographs and LIDAR imagery. The most important feature is the *main scarp*, which marks the upper boundary of a landslide. This feature is created where slide material is separated from the coherent material. Another important feature of landslides, especially deep-seated slides, is the benched topography, which results from the slide breaking into several components as it moves downslope. The final

important feature is the *toe* of the landslide, which marks the lower boundary of moved material.

## **Landslide Causes**

Shallow landslides are commonly caused by the buildup of pore water pressures in the soil mantle during periods of heavy precipitation and/or rapid snowmelt (Wieczorek, 1996). Deep-seated landslides often result from the percolation of water down through the upper bedrock or sediments to planes of weakness. Cruden and Varnes (1996) describe three processes that can cause landslides:

1. Increases in shear stress: increased shear stress results when lateral support is insufficient to maintain slope stability. Pertinent to this study, this may come in the form of the removal of support at the toe of a slide or the addition of weight to a steep slope. An example of the removal of lateral support could involve a river or wave cutting into the toe of a stable, inactive landslide, which might destabilize the slope. Constructing a new building on the edge of a bluff or saturating the ground by heavy precipitation can make a slope prone to failure by adding weight to a steep slope.

2. Low shear strength: low strength of the rock or soil material can make a slope prone to failure. The low strength may be the result of physical characteristics of the specific medium or discontinuities within the soil or rock mass (Cruden and Varnes, 1996). For example, joints or faults within a medium represent areas of low shear strength where further movement will likely be concentrated. Bedding planes in stratified sediments (clays) are weak, where as massive till is strong.



3. Reduced shear strength: reduced shear strength refers to the loss of cohesion of a material. An example of this process is the hydration of clay minerals, which results in a loss of cohesion. The loss of cohesion creates a situation where the clay particles readily slip past one another, which can lead to landsliding. Another process by which shear strength is reduced is an increase in pore water pressures at the boundary between two units. For example, if a permeable sandy unit overlies an impermeable clay unit, periods of high precipitation will result in the percolation of water through the sand. Water will pool when it reaches the impermeable clay. Pore water pressure increases at the boundary, decreasing the shear strength, and increasing the potential for sliding.

The downslope movement of geologic materials may be triggered by a number of natural factors including intense rainfall, rapid snowmelt, water-level change, wave or stream erosion, earthquake shaking and/or volcanic eruptions (Wieczorek, 1996). Human actions, such as the rerouting and/or concentration of water on a slope, placement of non-engineered fill material on the head of a slope, and man-made cuts into the toe of a slope can all increase the likelihood of future landslide activity (Hofmeister, 2000).

### **Stages in Landslide Evolution**

Gryta (1975) offers a useful framework for landslide evolution and field identification. He describes three stages of landslide evolution: (1) the initial stage, in which causal factors (increases in shear stress, low shear strength, and reduced shear strength) operate to create unstable conditions; (2) the advanced stage, in which landsliding takes place; and (3) the post-movement stage in which a slope is temporarily or permanently stabilized as a result of displacement of debris.

## **Landslide Mitigation**

Landslides pose a serious economic and social risk. By avoiding areas of known landslide potential, or by mitigating the damage potential, careful development of hillside slopes can reduce these losses. Kockelman (1986) proposes four ways to reduce landslide risks: (1) restriction of development in landslide-prone areas; (2) codes for excavation, grading, construction, and landscaping; (3) physical remediation measures (drainage, slope-geometry modification, and structures) to prevent or control landslides; and (4) development of warning systems. This study is especially important to the first step of Kockelman's approach. By identifying both the extent of individual landslides as well as slopes that are prone to future landslide activity civic planners can responsibly avoid landslide-prone regions. Landslide hazard maps offer these planners a tool with which to identify landslide prone areas. This study focuses on areas with present or ancient downslope movements. Previous landslide activity is often a very strong indicator for future slope instability (Wegmann et al., 2001).



## METHODS

Aerial photographs and LIDAR imagery were used to create independent landslide inventories for the 8km study area along the western shore of Kitsap Peninsula. The field area was divided into two sections (Figure 10). In section one, aerial photographs were used first to create an inventory and then an independent inventory was created with the LIDAR imagery. In section two, LIDAR imagery was used first and then the area was followed up with aerial photographs.

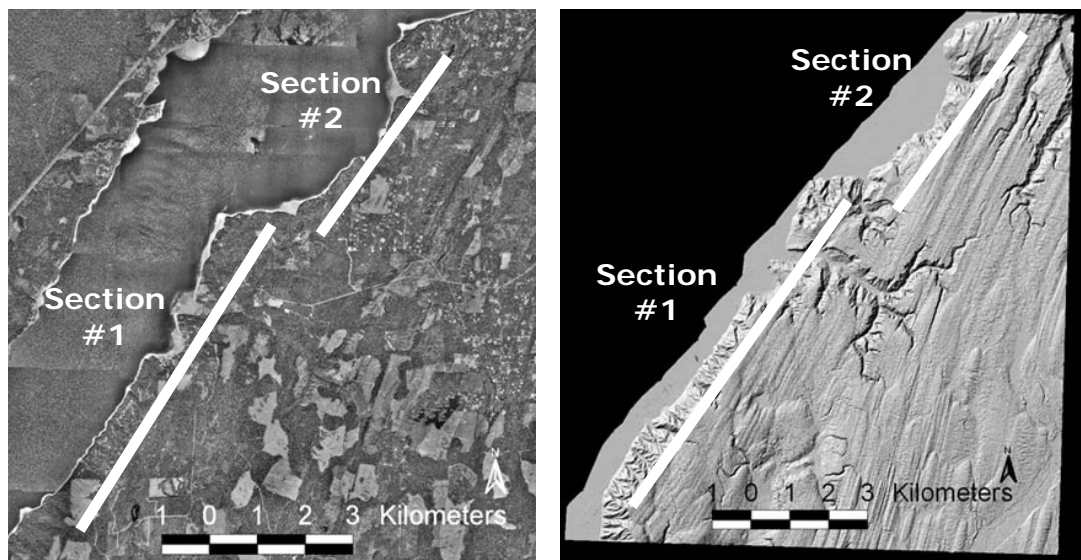


**Figure 10:** Field area with both types of images—orthophotograph (left) and LIDAR (right). Field area is divided into two sections. In section #1, aerial photographs were used first to create the landslide inventory and then followed with LIDAR interpretation. In section #2, LIDAR imagery was used first and then followed with aerial photograph interpretation.

### Aerial Photographs

Aerial photographs are taken from an aircraft flying in a straight line at a constant altitude above a selected region. The photographs are an “instantaneous record of the ground details as determined chiefly by the focal length of the camera lens, the flying height of the airplane at the time of exposure, and the film and filters used” (Ray, 1960,

p. 2.). A camera is mounted to the aircraft, aimed vertically down to the ground surface. Pictures are taken at regular intervals, such that each photo overlaps with the previous and subsequent photos (Figure 11). The film is then processed and printed on sheets of 27x27-centimeter photo-quality paper and numbered in the order of the flight line. A map is created for each set of aerial photographs, which geologists can access to determine which photos cover their particular field area.

For this study, aerial photographs were obtained from the Department of Natural Resources Photo and Map Sales Division. They included the following flight projects: JK-72, MLM-73, SP-85, SP-89, OL-95, and OL-97. Occasionally certain photos were missing from the collection, but with six sets of photographs, there are at least two different sets of photos that

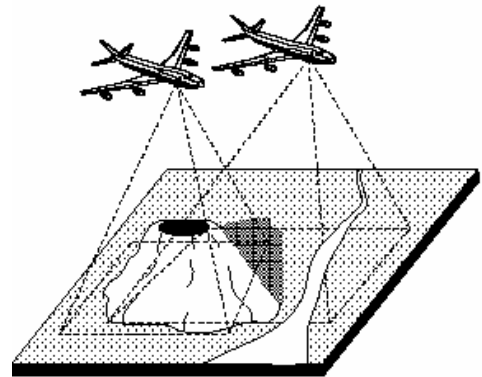


**Figure 11:** Aerial photograph acquisition (modified from Greely et al., 1998).

covered each portion of the study area. The aerial photographs were full stereo, with a scale 1:12,000, and were taken on north-south flight lines with a camera with a 12-inch focal (T. J. Curtis, oral communication, 2003). A single aerial photograph used for the study covers approximately 2.6 km<sup>2</sup>.

Aerial photographs are viewed in pairs. They are laid out in order such that the lower numbered photo (farther south) is on the left and the higher numbered photo (farther north) is on the right. They are oriented in the same direction and then can either be viewed through a stereoscopic device or with the naked eye. The image produced from the two side-by-side photos is a single “in-stereo” view of the ground surface:

topographic relief is evident. A Topcon mirror stereoscope was used to produce a high quality, magnified stereo-view of the field area with the following magnification options: 1x, 1.5x, 3x, and 6x (Figure 12). For mapping purposes, the photos were overlaid with transparent acetate paper and potential landslide features were delineated with colored pencils. For a detailed description of the methods and technology behind the production and use of aerial photographs, refer to Ray (1960).

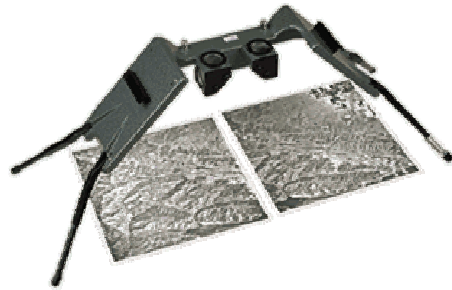


**Figure 12:** Stereoscope with pair of aerial photographs in field of view (modified from Greely et al., 1998).

Several topographic and geomorphic clues were evident in the aerial photographs that were used to identify landslides in the study area. In looking for deep-seated slide features, the most important feature was the classic, arcuate bowl-like shape with a steep face representing the main scarp (Figure 17). Debris and fallen trees on the beach as well as non-vegetated bluffs were often excellent clues for shallow landslides (Figure 20a). This was especially effective for aerial photographs that were taken following seasons of above normal precipitation—for instance, the 1997 photos. Another method employed was to look for man-made structures in various photo years. Occasionally, structures that were visible in an earlier photo were no longer visible in later photos—perhaps indicating that a geologic process such as a slide or flood event destroyed the home.

### **LIDAR Imagery**

Airborne LIDAR (LIght Detection And Ranging, also known as ALS—airborne laser scanning or ALSM—airborne laser swath mapping) is used to produce highly

detailed topographic images of the ground surface using low-flying aircraft and an onboard scanning laser rangefinder. LIDAR uses the same principle as radar. The LIDAR rangefinder transmits light out to a target, which is then reflected back to the rangefinder (Figure 13). The time that it takes for the light to travel out to the target and back to the rangefinder is used to determine the range to the target (Haugerud and Harding, 2001). LIDAR differs from radar in that it uses radiation that is at wavelengths that are 10,000 to 100,000 times shorter than that used by conventional radar



**Figure 13:** LIDAR data acquisition with rangefinder installed in fix-winged aircraft (modified from PSLC, 2000).

(Kavaya, 1999). The shorter wavelengths allow for the distance to the target to be computed with higher resolution. There are three main types of LIDAR including LIDAR range finders, differential absorption LIDAR, and Doppler LIDAR. A LIDAR rangefinder was used to survey Kitsap County.

For this study, the LIDAR images were paid for and provided by the Puget Sound LIDAR Consortium (PSLC). The PSLC contracted with an independent firm to produce LIDAR images of the ground surface in the Puget Lowland. An Inertial Measurement Unit (IMU) and GPS receiver located on the airplane provide for real-time spatial positioning of the aircraft in relation to the ground surface. The time interval between the laser pulse leaving the aircraft and the return of the reflected pulse back to the aircraft is measured precisely and then converted to distance. The aircraft and ground GPS data are used to accurately determine the aircraft longitude, latitude and altitude. The IMU

determines aircraft roll, pitch and heading. By combining the LIDAR, GPS, and IMU data, accurate three-dimensional digital terrain models of the earth are created.

Haugerud and Harding (2001) offer the particulars of the LIDAR survey conducted on this study area:

“Puget Sound Lidar Consortium members have contracted with TerraPoint LLC for surveys using a laser altimeter that covers  $\pm 17^\circ$  from nadir using a rotating pyramidal scan mirror, produces a 0.9m diameter laser beam on the surface, and records up to four returns for each laser pulse with a constant-fraction discriminator pulse detection scheme. The survey is designed to yield a uniform distribution of laser pulses across a 600 m swath across-and along-track spacing of 1.5 m. A 50% minimum side-lap between swaths ensures that all areas are covered at least twice, leading to an average pulse density of about  $1/\text{m}^2$ . All data are collected in winter months to maximize ground returns. The Consortium is purchasing all-return data, classified bare-earth returns, a bare-earth surface model, and a first return surface model. All data are delivered in State Plane projection with English units. Surfaces are gridded to 1.8 m (6ft) cells” (p. 1)

Simply put, the laser rangefinder fires approximately 30,000 points per second at the ground surface, getting returns with roughly 15 cm accuracy and approximately one data point for each square meter of the ground surface.

The laser pulses reflect off of all solid features including the forest canopy (branches, leaves, bushes, etc...), man-made structures (homes, roads, and other infrastructure), and the ground surface. The data is recorded and stored by the laser range finder in conjunction with the aircraft’s position relative to the ground surface. The ultimate result is millions of XYZ coordinates from numerous returns—some from the ground and some not.

Accurate landslide location can best be accomplished through a detailed image of the bare-earth surface—where the sliding is actually taking place. This requires the removal of factors that block the view of the bare-earth, which leads to the next step in processing the LIDAR data—the production of detailed digital elevation maps (DEMS)

of the bare-earth surface from millions of data returns that include laser returns from the forest canopy, man-made structures, and the ground surface. As Haugerud and Harding (2001) state, this process is not simple. For the data used in my study, Haugerud and Harding used powerful computers running many iterations of an algorithm designed to filter out the non-ground returns. For a complete discussion of the process involved in this "despike" algorithm, refer to Haugerud and Harding (2001). The ultimate product from the PSLC's work is a "clean," high-resolution image of the bare-earth surface from which this study was conducted..

The PSLC provided a copy of their bare-earth data. The data came in the form of Grid files (Digital Elevation Model (DEM) grids with a grid spacing of 2 meters) in five tiles: q471122e81be, q47122e82be, q47122e83be, q47122e84be, and q47123e14be. The data were processed with the computers and software available at the DNR-DGER. The main pieces of software used were ArcInfo, ArcView, and ArcMap, which are related ESRI software packages used to work with georeferenced spatial data.

The first step in processing the LIDAR data was to merge the tiles provided by the PSLC into a single, coherent grouping of referenced data points. The data points were then converted into a GRID image, which connects data points with triangular planes that result in a coherent, geo-referenced image. Finally, the projection of the GRID was changed to State Plane South, North American Datum of 1927 (NAD27), which is compatible with the DNR's database of spatially referenced ArcInfo coverages including roads, streams, county lines, land use zoning, elevation contour, and other applicable themes. From the GRID image, contour lines were created from the LIDAR data in ArcInfo.

The final step to produce a useable product from the LIDAR data was to make hillshaded images from the reprojected GRID image. There are four components that can be controlled when producing hillshaded images: azimuth, altitude, shading, and z-factor. Different combinations of these components were assessed to determine the best combination for the identification of landslides.

The *azimuth* refers to the angle from which a light source is projected. It is expressed in positive degrees from 0 to 360, measured clockwise from the north. The default is 315 degrees, though for this study, a variety of azimuths in 30° increments varying from 45° to 255° were helpful to illuminate and accentuate morphologic features on slopes with different aspects (Figure 15a-f).

*Altitude* is the slope angle of the illumination source above the horizon. The slope is expressed in positive degrees, with 0 degrees at the horizon and 90 degrees directly overhead. The default is 45 degrees, which was used for this study.

The third component, *shading*, specifies the type of shaded relief to be generated and it considers both the azimuth and altitude illumination angles. The default is “ALL,” which means that the output grid contains values ranging from 0 to 255, with 0 representing the darkest areas and 255 the brightest.

The final component is the *z-factor*, or vertical exaggeration. The number of ground x,y units in one surface is a z-unit. ArcInfo allows the user to multiply the z-unit by any integer to control the exaggeration of relief and thus, shading. The default is  $z=1$ . For this study, a z-factor of 2 was used to double topographic relief.

Four sets of maps, each of which covered approximately a quarter of the field area, were created on a large plotter printer. For each of these sections, two maps, one



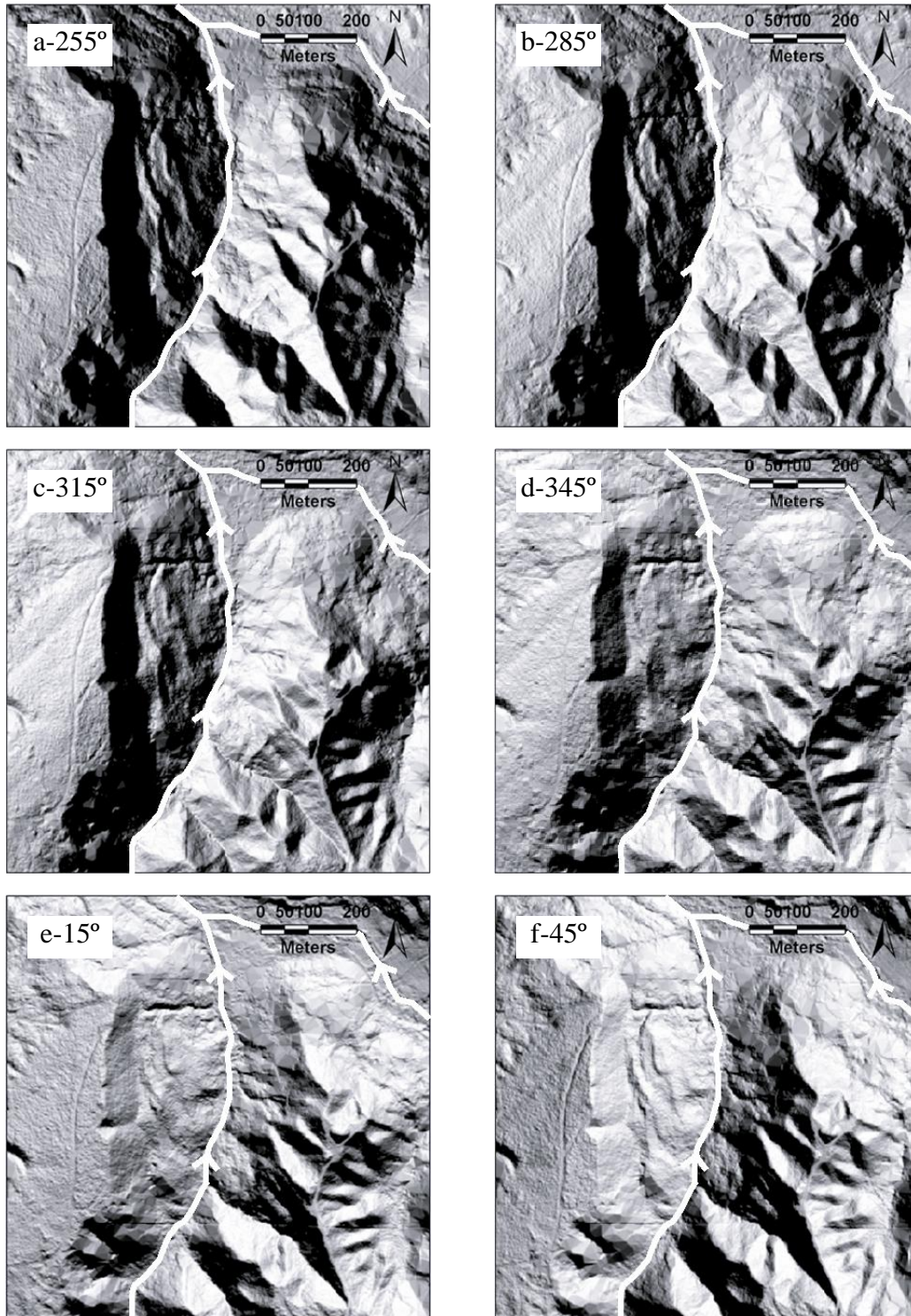


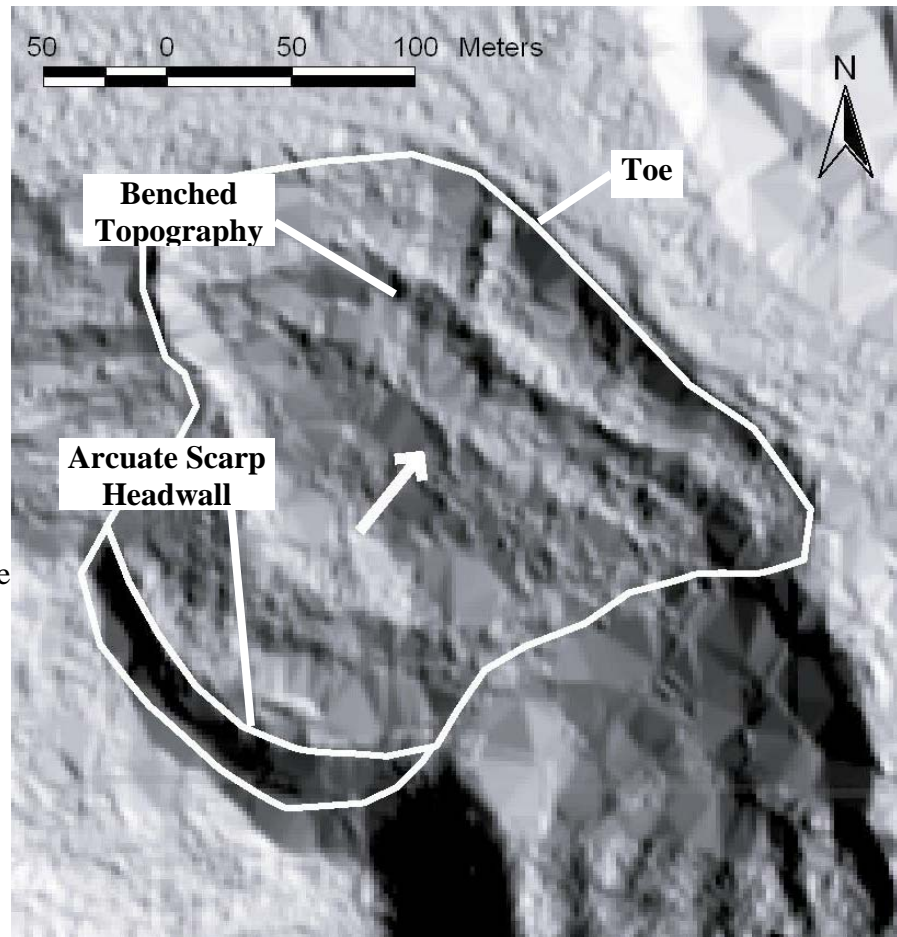
**Figure 14a-f:** Sun azimuth has a dramatic effect on the visibility of slopes in this tributary of Anderson Creek. Notice that east-facing slopes are completely in shadow when the sun comes from the west, whereas texture and definition is gained when the sun shines from the northeast. For example, in figure (e) with sun azimuth 15°, the east facing slope is well illuminated.



with a sun position of 315° and the other with a sun position of 45°, were created.

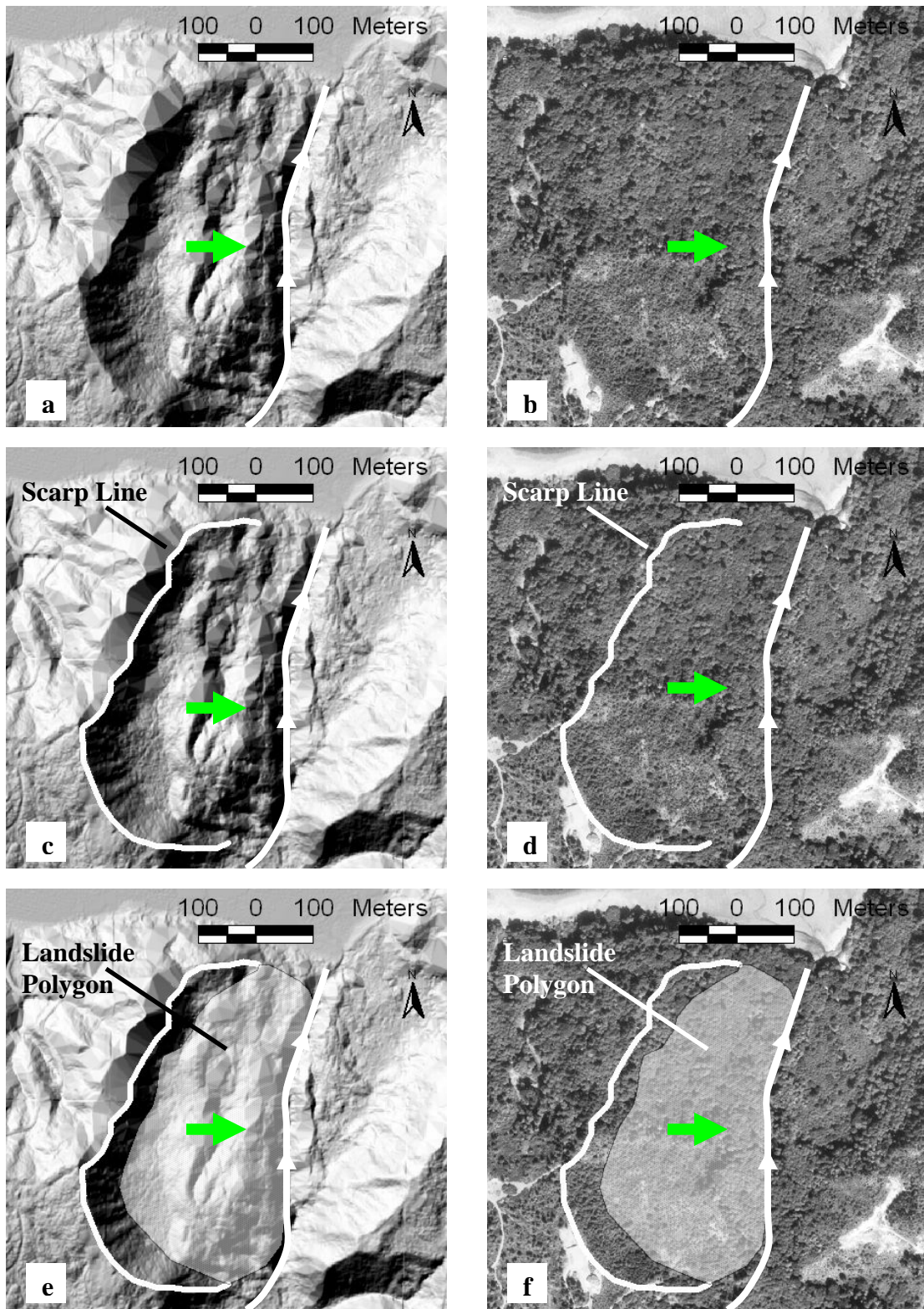
Colored pencils were used to indicate suspect slides. The most important features looked for were arcuate scarp headwalls, benched slide bodies, and the toes of the landslides (Figure 15). It took approximately three days to create a landslide inventory for the field area using this methodology.

**Figure 15:** This image depicts the typical slide features that indicate landslide activity. Notice the arcuate scarp headwall at the bottom of the picture and the benched topography that predominates downslope to the toe of the landslide (south side of Anderson Creek drainage).



## Digitization

After landslide inventories were created from aerial photographs and the LIDAR printouts, the landslides were digitized into an Arc project. A polygon was used to indicate the body of the landslide and a line to indicate the upper boundary of the scarp headwall (Figure 16a-f).



### *Orthophotographs*

For this project, DNR flight project OL-94 digital orthophotographs were used. Orthophotographs are a single image, flown at 13,277-meters Above Mean Terrain (AMT), using a 21-centimeter focal length lens. Source photography is at a scale of 1:63,360 (1-centimeter equals 0.63-kilometers) and the digital image has 1-meter pixel resolution (T. J. Curtis, oral communication, 2003). The image was ortho-rectified by the DNR photogrammetry department using full analytical aerial triangulation performed on the aerial imagery with a 30-meter DEM. The horizontal accuracy of these images is officially plus or minus 6-meters or better (generally better in my experience). For this study, the orthophotographs were geo-referenced and projected in State Plane South, NAD27.

From the DNR's Photo and Map Resources Department, three black and white digital orthophotographs were obtained: s72502w0, s72402w0, and s72403w0. The images were loaded into an Arc project, where two themes were created: "airphoto\_slides" "airphoto\_scarps." The landslide inventory from the aerial photographs was then digitized into the Arc project. Using the polygon drawing tool, the body of the slides was indicated in the theme "airphoto\_slides". The line drawing tool was used to indicate the area between the slide and the top of the scarp headwall in the theme "airphoto\_scarps" (Figure 16). The entire process took approximately four days.

Because the orthophotos are a single image, they are not in stereo. Therefore, it was sometimes difficult to locate specific drainages and other topographic features discernable on the stereo aerial photograph pairs. It was helpful to use contour lines from the DNR's database, superimposed on the orthophotos, to locate features.

### *LIDAR*

The process for digitizing the slides located on the LIDAR images was similar to the process used with the aerial photographs. Two themes were created within the Arc project, "lidar\_slides" and "lidar\_scarps." Landslides were digitized from the slides delineated on the LIDAR printouts. The body of landslides were indicated with the "lidar\_slides" polygon theme and the scarp headwalls with the "lidar\_scarps" line theme (Figure 16). The entire processes took approximately two days.

### **Field Methods**

With such a large field area, it quickly became evident that it was not possible to verify each of the slides identified on the LIDAR and aerial photographs. It was determined that detailed surveys were best conducted near those areas with more extensive development. These include the development near Chinom Point, the town of Holly, and the bluffs near Tekiu Point. For the remainder of the less-developed portions of the field area a less thorough survey was conducted.

Following Gryta's (1975) criteria for the state of activity of landslides and criteria for distinguishing shallow and deep-seated landslides, 11 days in the field were spent in the field verifying landslides previously identified on aerial photographs and LIDAR

imagery. United States Geological Survey topographic maps, as well as maps created in Arcview that showed identified slides on aerial photographs and LIDAR, were relied upon. The following tools and methods were used in conducting on-the-ground verification surveys:

#### *GPS unit*

A hand-held Garmin V Global Positioning System (GPS) instrument was used to record the location of slides, important outcrops, and photographs. Waypoints were collected in decimal degrees utilizing the World Geographic System Datum of 1984 (WGS84). Waypoint accuracy was generally  $4.5 \pm 1.5$  m. The waypoints were downloaded from the Garmin to a desktop computer, at which point they were reprojected from WGS84 into Washington State Plane South, NAD27 format and imported into the Arc project.

#### *Water access*

An Old Town Discover 163 Series polyurethane canoe was used for a large portion of the fieldwork in order to gain easy access to slide areas near the water. A small, Minn Kota Endura-40 electric boat motor was attached to the rear of the canoe, which provided locomotion power.

#### *Camera*

A Nikon Coolpix 990 digital camera with a Wide Converter WC-E63 0.63x wide-angle lens was used to record images of the study area.

### *Traverses*

In addition to accessing slides from the water, many of the slides were accessed from logging roads. From these roads, large sweeping traverses were made of slopes with suspected landslides.

### *Landslides*

As previously described, landslides were distinguished as either shallow or deep-seated (p 13).

The three stages of activity used to classify slides in the study are *active*, *young*, and *dormant*.

1. The criteria for an *active* slide are the following: (a) unstable slopes, (b) the presence of a bare scarp, (c) the presence of terraces and minor slump units, (d) an alteration of the orientation of trees, and (e) the presence of toe debris (Gryta, 1975).
2. The criteria for a *young* slide are the following: (a) the presence of a main scarp with young vegetation patterns, (b) the presence of hummocky ground with mildly subdued features, and (c) the presence of strongly bowing or pistol-butt tree trunks.
3. The criteria for a *dormant* slide include the following: (a) a scarp headwall that is heavily vegetated, (b) the presence of very subdued hummocky topography, and (c) the presence of mildly disoriented tree trunks.

## DATA & RESULTS

After landslide inventories were created from both types of imagery and after the field verification portion of the study, data were analyzed to compare the two types of imagery.

From the aerial photographs, 97 landslides were identified (Table 1). Of these slides, 51 were field verified. Based on field verification and a comparison with the inventory created from the LIDAR imagery, it is determined that 59 of the 97 slides were “real.” A “real” landslide is one that has enough evidence to warrant including it in the final landslide inventory created for the field area (Plate 1).

| Table 1: <b>Aerial photographs</b> |    |
|------------------------------------|----|
| Number of Slides Identified        | 97 |
| Number Field Checked               | 51 |
| Number of REAL A.P. Slides         | 59 |

From the LIDAR imagery, 83 landslides were identified (Table 1). Of these slides, 52 were field verified and based on this field verification as well as a comparison of the inventory created from the aerial photographs, it was determined that 50 of the 83 landslides were “real.”

| Table 2: <b>LIDAR</b>       |    |
|-----------------------------|----|
| Number of Slides Identified | 83 |
| Number Field Checked        | 52 |
| Number of REAL Lidar Slides | 50 |

A total of 86 “real” landslides were identified from the LIDAR imagery, the aerial photographs, and the field verification (Table 3). Seventy-two of the slides were field checked. Of these slides, 17 were identified on the LIDAR imagery only, 26 on the aerial photographs only, and 33 on both the LIDAR and the aerial photographs. Ten of the



slides were identified in the field only, and not located on either LIDAR or aerial photographs.

|   |           |
|---|-----------|
| <b>Table 3: Total Real Slides</b>           | <b>86</b> |
| Number of Slides Identified on LIDAR only   | 17        |
| Number of Slides Identified on A.P. only    | 26        |
| Number of Slides Identified on A.P. & LIDAR | 33        |
| Number of Slides Identified only in Filed   | 10        |
| Number of Slides Field Checked              | 72        |

Slides in this study were classified as either shallow or deep-seated (Table 4). Of the 40 total shallow slides, 15 were identified on LIDAR imagery and 28 were identified on aerial photographs. Of the 46 total deep-seated landslides, 35 were identified from LIDAR imagery and 30 from aerial photographs.

|  |    |
|--|----|
| <b>Table 4: Shallow and Deep-Seated Slides</b> |    |
| Total Shallow Slides                           | 40 |
| Total Deep-Seated Slides                       | 46 |
| Shallow Slides Identified on LIDAR             | 15 |
| Shallow Slides Identified on A.P.              | 28 |
| Deep-Seated Slides Identified on LIDAR         | 35 |
| Deep-Seated Slides Identified on A.P.          | 30 |

Table 5 compares where in the field area landslides were identified (Figure 4). In the southern portion of the field area where pre-Vashon gravel (Qpg<sub>o</sub>) dominates, all 18 of the slides identified were shallow. Farther north, where interglacial beds (QPS) are overlain by pre-Vashon gravel (Qpg<sub>o</sub>), 3 of the 4 slides were shallow and only 1 was deep-seated. Continuing north, the pre-Vashon gravel (Qpg<sub>o</sub>) pinch-out. They are replaced by advance outwash deposits (Qgas) that overlie interglacial beds (Qps). In this area, 19 of the 61 slides are shallow, whereas 42 are deep-seated. At the northern portion of the field area, where the interglacial beds (Qps) disappear and advance outwash (Qgas) dominates, all 3 of the slides are deep-seated.



| Table 5: <b>Slide Type and Location</b>   |    |
|---|----|
| Slides occurring at southern portion of field area in pre-Vashon gravel (Qpg <sub>o</sub> )                                     | 18 |
| Shallow   | 18 |
| Deep-Seated   | 0  |
| Slides occurring south of Holly at contact between pre-Vashon gravel (Qpg <sub>o</sub> ) and interglacial beds (Qps)            | 4  |
| Shallow   | 3  |
| Deep-Seated   | 1  |
| Slides occurring in center portion of study area at contact between advance outwash deposits (Qgas) and interglacial beds (Qps) | 61 |
| Shallow   | 19 |
| Deep-Seated   | 42 |
| Slides occurring in northern portion of study area in advance outwash deposits (Qgas)   | 3  |
| Shallow   | 0  |
| Deep-Seated   | 3  |

## DISCUSSION

### **Interpretation of How LIDAR Imagery and Aerial Photographs Compare**

Overall, slides inventories created from LIDAR imagery were about as accurate (real) as the slides defined from stereo pairs of aerial photographs. This conclusion is based upon the field verification of landslides identified from both types of imagery. A total of 97 slides were identified from aerial photographs. Of these, 60% were determined to be real (Table 1). A total of 83 slides were identified from LIDAR imagery. Of these 60% were determined to be real (Table 2). This suggests that neither method is significantly better or worse than the other for total success in locating landslides. However, a more holistic view that accounts for factors like the type of slide, the precision of landslide delineation on a map, vegetation, efficiency, required technology, required training, availability of the data, and the interval between data acquisition, reveals that each method offers users distinct pros and cons.

Both LIDAR imagery and aerial photographs afford geologists different advantages and disadvantages when looking at slope instabilities. Through a discussion of the strengths and weaknesses of both methods, it will be demonstrated that the use of both techniques in combination offers geologists the most powerful remote sensing package. Again, it is important to emphasize that areas of past landsliding usually correspond with future landslide events. Therefore, the identification of past landslides can help with mitigation decisions and future land use planning.

### *Type of slide*

The ability to accurately and precisely identify and define slides is greatly controlled by the type of slide and its state of activity. Thirty-five real, deep-seated landslides were identified using LIDAR imagery and 30 of this type of slide were located on aerial photographs (Table 3). In general, these deep-seated slides are highly visible on the LIDAR imagery and usually visible on aerial photographs (Figure 17). The large

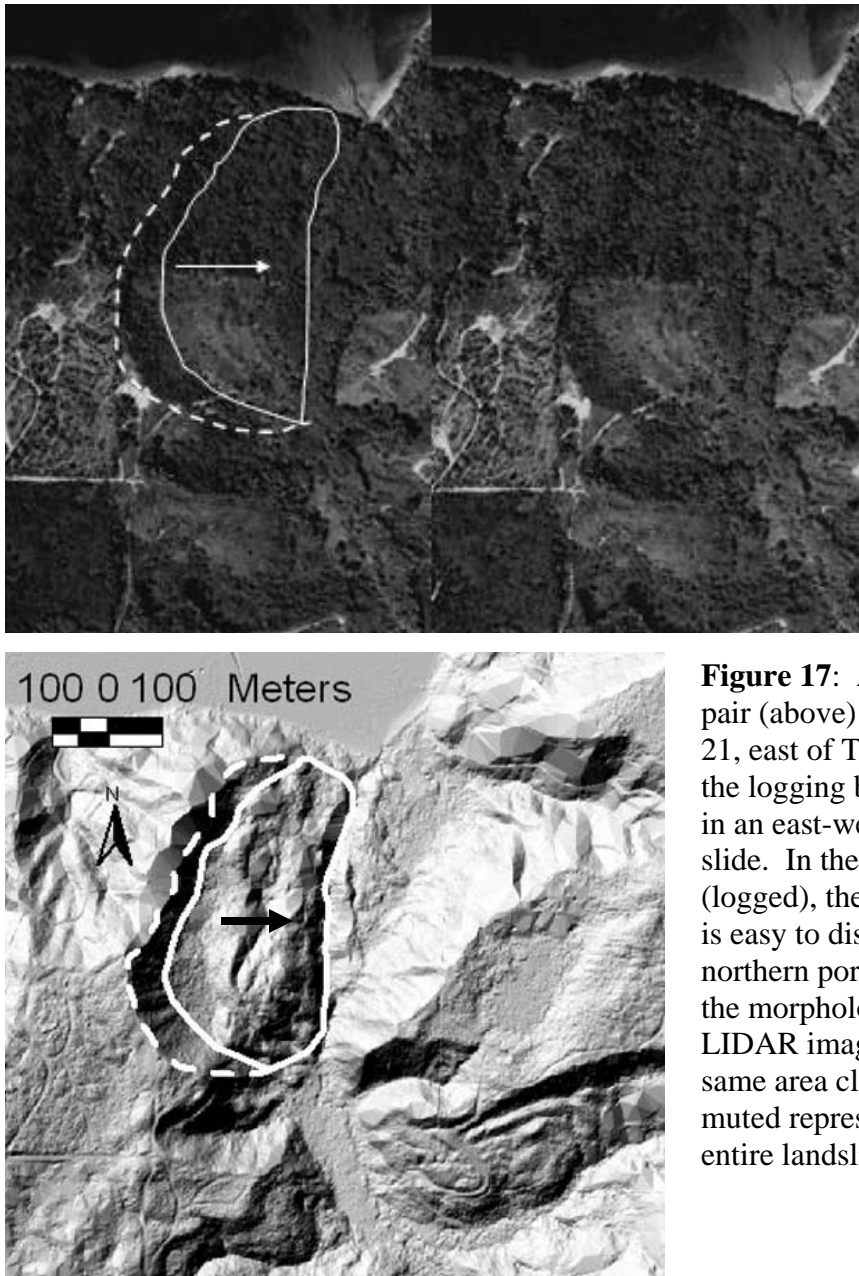


**Figure 17:** Aerial photograph pair (above) depicts landslide 21, east of Tekiu Point. Note the logging boundary that cuts in an east-west line across the slide. In the southern portion (logged), the slide morphology is easy to discern, but in the northern portion (vegetated), the morphology is muted. The LIDAR image (below) of the same area clearly shows an unmuted representation of the entire landslide body.

slide features are readily visible on LIDAR because the resolution of laser returns is high enough to show the detailed morphology of the slides. For aerial photographs, the resolution is also high enough to locate these features.

Shallow, smaller slides, which are especially present in the southern reaches of the study area, were much more easily identified on aerial photographs than on LIDAR imagery. Only 15 slides were identified from LIDAR imagery, whereas 28 of a total 40 real slides were identified from aerial photographs (Table 3). This huge discrepancy suggests that LIDAR imagery does not work well for locating shallow features—likely a result of too coarse a resolution and also because vegetation cues often help to locate these slides. Landslide 86 (Plate 1) near Hood Point offers a useful example for illustrating the difference between LIDAR and aerial photographs (Figure 20). On the aerial photograph, notice debris at the beach level as well as a slight depression in the slope. On the LIDAR image, the debris has been filtered out of the image and the resolution is too coarse to distinguish the depression on the slope as a distinct feature that suggests slope movement.

### *Precision*

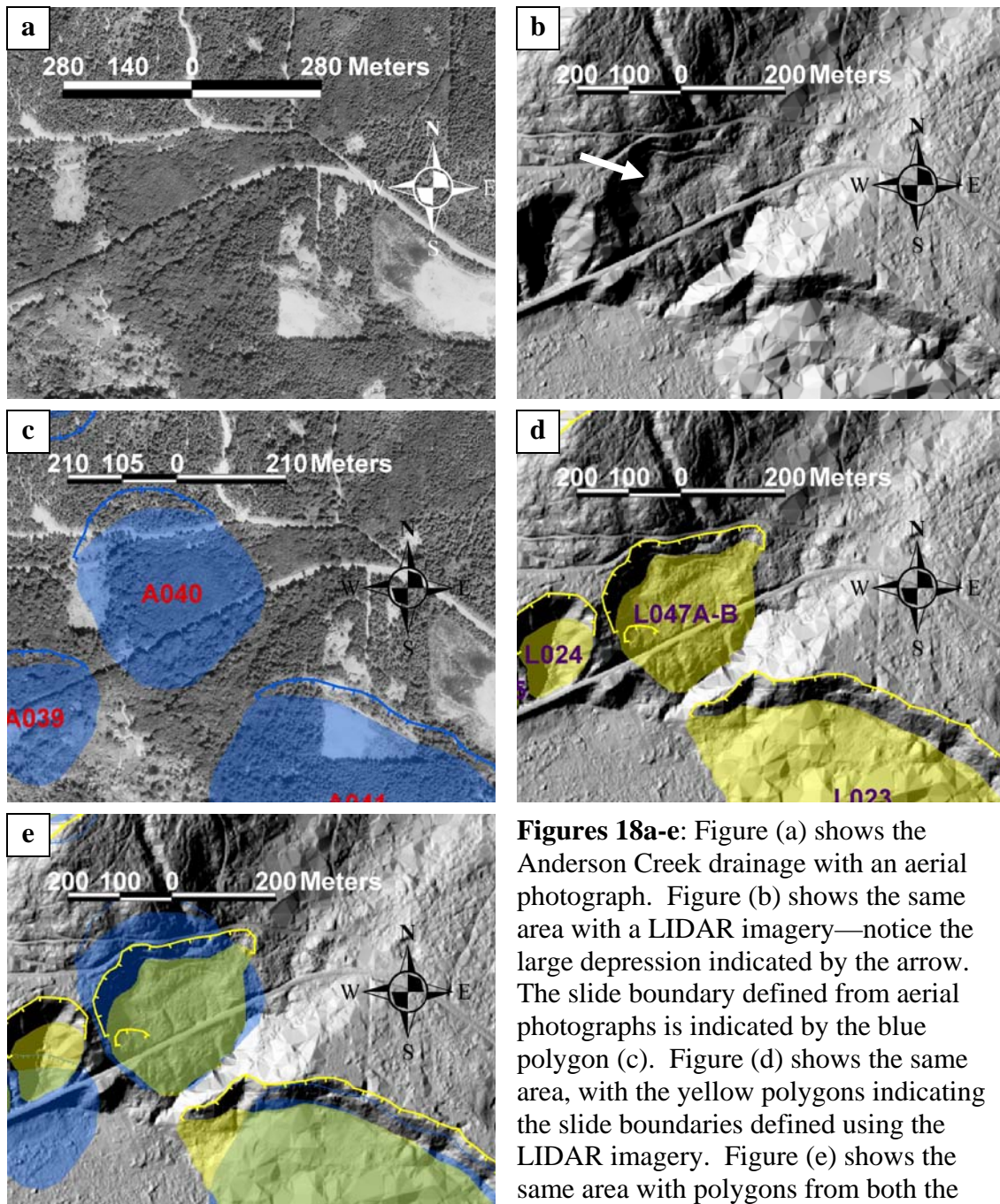
Precisely defining the boundary of a slide is a crucial step in the creation of a landslide (or slope stability) hazard zonation map. The spatial location of slide boundaries on landslide inventory maps can have a profound impact on future land-use planning and ultimately land utilization decisions. For example, slide boundaries might affect where future roads are built, whether permits are issued to residents seeking to construct homes, or might even adversely affect property values. In general, more

precise spatial location of slide boundaries was obtained from the LIDAR imagery compared to the boundaries assigned from aerial photographs.

Landslide 24 (Plate 1) in the Anderson Creek drainage provides an excellent example of how the use of LIDAR imagery is more precise in defining spatial landslide boundaries. It is difficult to notice subtle ground morphology on the orthophotograph (Figure 18a), but the LIDAR imagery in Figure 18b clearly reveals the geomorphic features of the slope. The arrow indicates a depression with hummocky topography below the scarp headwall. Figure 18c shows the area delineated with slides from the aerial photographs—indicated by blue polygons. Figure 18d shows the same area with LIDAR imagery with a yellow polygon covering the landslide boundary previously defined on the aerial photographs. Figure 18e shows both polygons overlying each other on the LIDAR imagery. In this figure it is very apparent that precise landslide boundary definition is better attained from LIDAR imagery. Figure 19 shows this area from the ground with Steve Palmer acting as scale, standing next to a scarp wall within this slide complex.

Several factors contribute to poor precision from the aerial photographs. One key factor is that while the slides are identified in-stereo, they are digitized and defined on a computer monitor displaying a flat image. Thus, the relief is lost and the cartographer is forced to rely on locating reference points on the stereo photograph pairs and then matching them with the same points on the “flat” digital orthophotographs. Even with the help of contour lines, it was a difficult, tedious, and ultimately imprecise method.

Another factor contributing to the poor precision on the aerial photos is the effect of vegetation muting landslide boundaries. While it is often obvious that sliding has



**Figures 18a-e:** Figure (a) shows the Anderson Creek drainage with an aerial photograph. Figure (b) shows the same area with a LIDAR imagery—notice the large depression indicated by the arrow. The slide boundary defined from aerial photographs is indicated by the blue polygon (c). Figure (d) shows the same area, with the yellow polygons indicating the slide boundaries defined using the LIDAR imagery. Figure (e) shows the same area with polygons from both the LIDAR and aerial photographs. Notice that the yellow slide boundaries have much greater precision. In this figure, the blue, boundaries boundaries derived from aerial photographs creep far past the actual slide boundaries.





**Figure 19:** Field partner, Steve Palmer, standing next to scarp of landslide 29. The precision was much better with LIDAR imagery than with the aerial photographs.

recently occurred, for instance from obvious depressions or downed trees, vegetation masks the precise boundaries of the slides, leading to imperfect precision.

A final problem with the methodology used in this study is that none of the aerial photographs were taken during the same year as the orthophotographs. Therefore, distinct features (especially vegetation cues) that were present on an aerial photo pair were not always visible on the orthophotographs; thus complicating the transfer of landslide locations from aerial photographs to the digital orthophotographs.

### *Vegetation*

Vegetation works both for and against landslide location. Vegetation cues, especially on slopes with shallow landslides, often aid in slide location. Conversely,

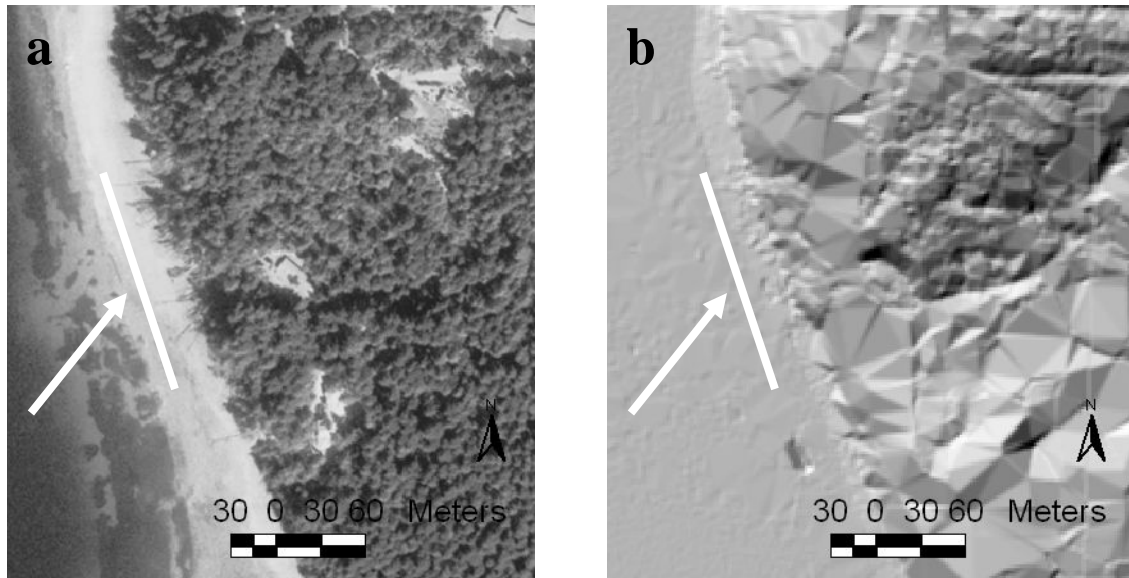
vegetation mutes the topography of the ground surface, interfering with key geomorphic features that might indicate slope movement.

One distinct advantage to using aerial photography to locate landslides is the clarity of vegetation cues (heavily debris-laden beaches and listing trees). Throughout the study area, beach areas with high concentrations of debris (mainly downed trees) often indicated recent slope movement and deposition of slide debris and trees within the intertidal zone. It is easy to identify debris-laden beaches on photo sets that were flown after winters with particularly heavy precipitation (the 1997 photos). Figure 20a shows downed trees on aerial photographs that are not present on the LIDAR imagery (Figure 20b). Figure 20c confirms the landslide with field verification—notice the debris on the beach.

While vegetation cues can help in locating landslides, foliage can also mute ground morphology and hinder landslide identification. For example, logging patterns can be confusing to the untrained eye. At a clear-cut logging boundary, the difference in elevation between the tops of older trees and the ground level of an adjacent newly clear-cut area can be very large—up to 20 m. The change in elevation can trick the eye into seeing huge drops in slope, where the ground is actually level. This problem is exaggerated in areas where a logging pattern is arcuate, suggesting a scarp headwall.

Vegetation also masks subtle changes in topography. Tall and dense vegetative cover can mute areas characterized by hummocky topography, one of the indicators of landslide movement. On aerial photographs, there is no way to penetrate the vegetation, which leaves the geologist guessing as to the true ground morphology below the tree canopy.





**Figures 20a-c:** Figure (a) shows an area just south of Hood Point with many downed trees due to landslide activity above the beach. These trees were used as indicators of active sliding. Figure (b) shows the same area with LIDAR imagery. The LIDAR imagery is not of a high enough resolution to show the trees and without them, there is no indication of sliding in the area. Figure (c) is a picture taken from a canoe looking at the slide. It is a real slide, that is fairly shallow.



The huge advantage of LIDAR imagery over aerial photographs is that a computer algorithm is able to strip away the vegetation, revealing a digital image of the bare-earth surface. Working under the assumption that the virtual deforestation algorithm

produces an accurate image of the bare-ground, this capability is extremely powerful. No longer do geologists have to attempt to “see through” the tree canopy to guess what sorts of landforms actually exist; the computer takes away the guessing. The capability to “see through” the vegetation has exciting possibilities. Notice the esker and the trellis drainage pattern in Figure 21. These landforms can be very difficult to see with photogrammetric approaches, but in areas of good laser return the detail is astonishing.

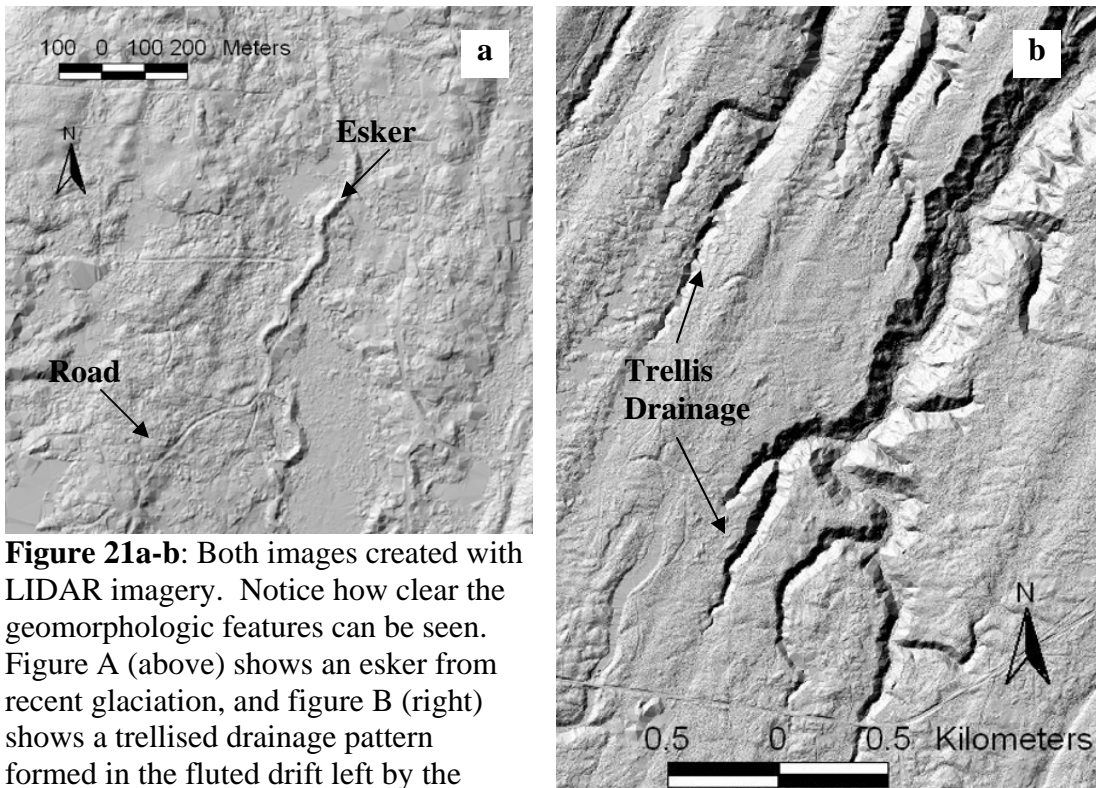


**Figure 21a-b:** Both images created with LIDAR imagery. Notice how clear the geomorphologic features can be seen. Figure A (above) shows an esker from recent glaciation, and figure B (right) shows a trellised drainage pattern formed in the fluted drift left by the glacier.

There are distinct advantages to using LIDAR imagery for landslides identification. Landslide 29 (Plate 1) serves as an excellent example to show the advantages of LIDAR. Refer back to Figure 17, which depicts this landslide on an aerial photograph pair and LIDAR imagery. There is a logging boundary that cuts across this slide. In the southern portion, which has been logged (vegetation removed), the

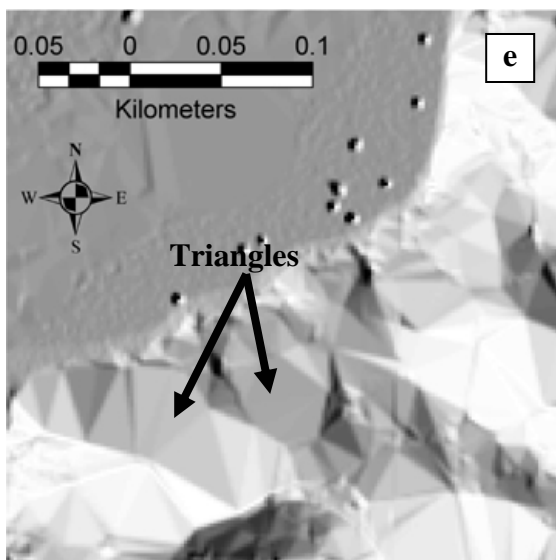
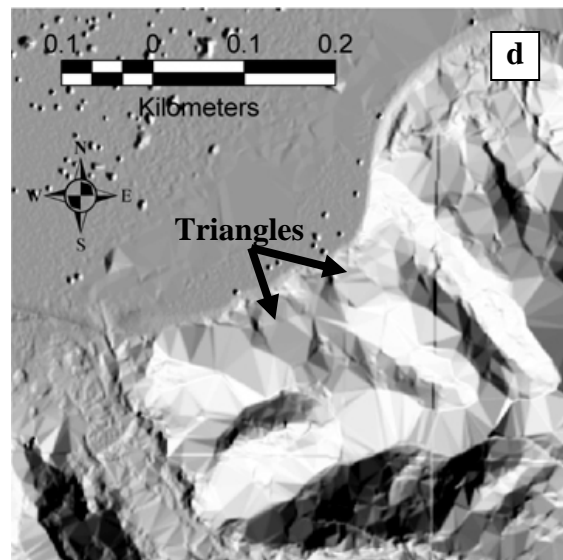
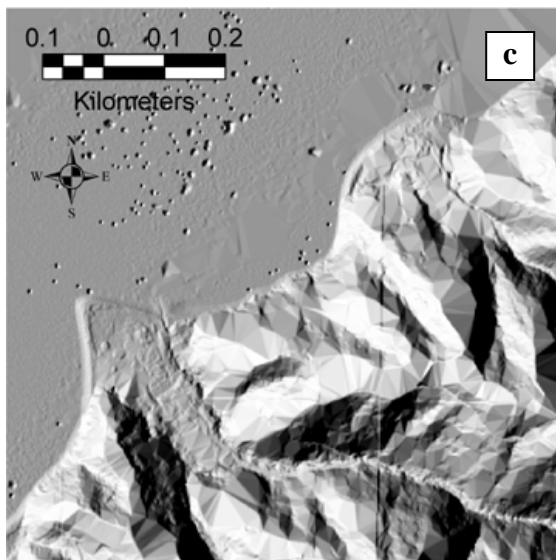
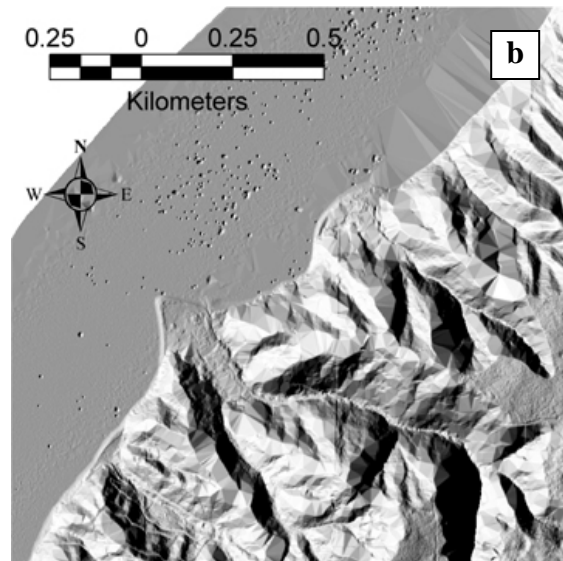
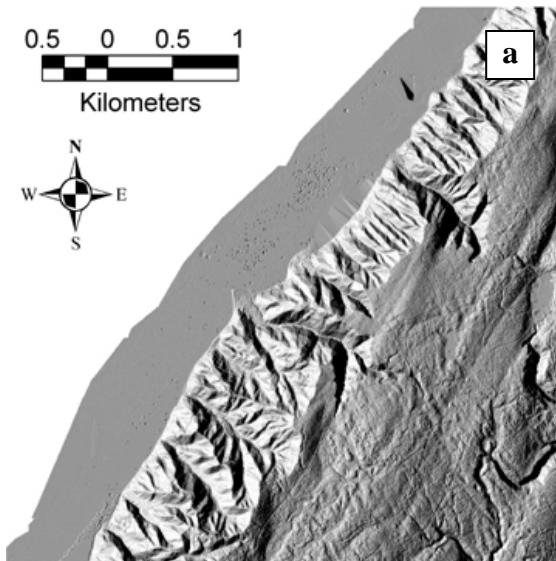
morphology is readily visible on the aerial photograph pair. Morphology is muted in the northern portion that is vegetated. On the other hand, LIDAR imagery shows this landslide in great detail on both the northern and southern portions of the landslide—a function of the digitally removed vegetation.

Unfortunately, “seeing through the trees” does not always work with LIDAR imagery. In areas with extremely dense canopy cover or on very steep slopes, the number of last-return laser pulses (presumably the earth’s surface as opposed to vegetative features within the forest canopy) is often poor, resulting in low-resolution imagery. The low resolution manifests itself as large triangles on the LIDAR imagery producing a faceted-appearance (Figures 22a-e). In the case of low densities of return laser pulses (commonly in areas with dense canopy cover or on steep slopes), LIDAR imagery is no better (perhaps even worse) than aerial photographs.

#### *Required experience/necessary training*

Prior to this study, I had some previous experience with aerial photographs, little experience with GIS software, and no experience with LIDAR imagery.

Aerial photographs require thorough training to gain proficiency in landslide identification. For a novice user, vegetation patterns can be confusing and topographic highs and lows are often inverted. Another problem for beginners is that the large quantity of photographs required to cover a study area can be difficult to manage. I found two techniques to be extremely helpful in developing my ability to use aerial photographs effectively. First, I found that it helped to draw drainages and ridges on the acetate paper that covered the photographs and then I compared my work to available



**Figures 22a-e:** At the larger scale (Figure a) the LIDAR image appears coherent and detailed. But as the image is magnified, the image becomes “triangulated” and difficult to interpret (Figures d & e).

topographic maps. The second technique involved working on a set of photographs from which a landslide inventory had already been created. I practiced finding slides on this set of photographs and then compared my work with the already completed inventory. After this training, I began work on the photographs that covered my field area. I regularly checked with Wegmann, who has had extensive experience with photogrammetric techniques and was able to guide my project. In summary, significant training is required to effectively use aerial photographs.

Conversely, I found LIDAR very easy for locating landslides. The hillshaded image gives the viewer an immediate sense of topographic relief. I required little training to locate simple landslide features on the LIDAR imagery and I believe that people who are untrained in photogrammetry can easily and quickly use LIDAR imagery.

### *Efficiency*

Another important aspect of remote sensing is the ease with which the geomorphic features can be transferred to a digital environment. After slides were identified with both methods, the boundaries of the features were digitized using the polygon and line tool in the Arc project.

For aerial photographs, this required transferring the slides from the aerial photographs to georeferenced orthophotographs. This technique was hindered by the fact that the transfer was from a stereo-image (pairs of photographs) to a flat image (orthophotograph). Working on the orthophotographs, difficulty was encountered in establishing slide locations and slide boundaries. Topographic contours from the DNR database were overlaid on the orthophotograph to help locate drainages and ridges to help

in this process, but even with this aid, some of the topography was too subtle to show up with definite boundaries on the orthophotographs. Confidence in transferring slides using this transfer method was low. The digitization process from the aerial photographs took approximately seven working days.

LIDAR imagery was much more user-friendly for the digitization process. Transferring slide boundaries into the Arc project was a simple process because the exact image used in defining the spatial extent of individual slides was visible on the computer screen. Both images were hillshaded, so there was no question as to where to draw the boundaries. Greater confidence was felt with digitizing the landslides onto the LIDAR. For the LIDAR, the process took approximately three working days.

Beyond locating the slides on imagery, another important aspect of the study was the ability to make use of the imagery in the field. After eleven days of landslide verification and mapping in the field, it was found that LIDAR imagery is significantly easier to manage for the following reasons: the LIDAR imagery is hill shaded, which gives the effect of being in-stereo; the LIDAR imagery was printed out on disposable paper, so getting the image dirty and wet was not a concern; and the LIDAR imagery was a single, coherent image as opposed to aerial photographs which are a series of small, disconnected images that must be constantly managed while moving around in the field.

Most field days required anywhere from eight to twenty aerial photographs to properly cover the ground surface. As location was changed in the field, aerial photographs constantly had to be switched to gain coverage of new areas, which was a time-consuming process. Another problem encountered was obtaining a stereo image in the field. While the ability to look at aerial photographs in-stereo with the naked eye was

developed, the amount of the magnification was very limited. In order to get magnification, a bulky stereoscope was required, which was not practical in the field. Therefore, trouble was encountered in confirming the specific features that were used to originally identify landslides. Another problem with aerial photographs is their intolerance to western Washington's wet climate. Several of field days were spent in the rain. Because the aerial photographs were on loan, they could not get wet, which was often awkward and time-consuming. The best way to manage the landslide inventory from aerial photographs was to use a printout of a contoured orthophotograph from the Arc project that included landslides previously defined from aerial photograph pairs in the office. The combination of the original aerial photographs, the contoured orthophotographs, and a topographic map was best for conducting landslide verification and mapping. However, it was not as efficient as with the LIDAR imagery.

### *Manipulation*

Another advantage of LIDAR imagery versus aerial photographs is the ease with which it can be manipulated. Aerial photographs are a "snapshot in time", in which variables like sun position, sun angle, and shadows cannot be changed. If the sun position creates shadows that obscure certain features, the only solution is to look at photographs from different years, which can be a time consuming and laborious process. LIDAR imagery on the other hand is infinitely manipulatable because it is digitally created. Therefore, factors such as sun position, sun angle, and shadows can quickly be changed. For the purposes of this study, it was found that the sun azimuth was the most important variable for viewing the LIDAR imagery. As discussed in the methodology

section, six hill shaded maps, with sun azimuths varying from 255° to 45°, were created. These images were imported into the Arc project, which allowed for easy viewing of multiple hill shaded images to clarify the morphology on specific slopes (Figures 14a-f).

#### *Interval between flights*

One distinct advantage to aerial photographs over LIDAR is their regular acquisition. Whereas LIDAR is still a relatively new technology and has only been flown once for Kitsap County, aerial photographs are flown regularly over the entire state of Washington. In Kitsap County, the photos have been acquired roughly every five years. This study used photographs from the past 30 years, which revealed changes in the morphology and vegetation of the region. This record was particularly advantageous for areas that have been logged: aerial photographs gave a detailed view of the true bare-earth surface. Also, the 30 year span of photographs helped to narrow down when landslides had occurred.

#### *Current standard in the field of geology*

Another factor to consider in comparing the two techniques is the duration for which they have been used in the field of geology. For western Washington, the air photo inventory extends back to the 1930s (R.J. Carson, oral communication, 2003). Techniques for using the photos have been refined and developed over the years and expensive equipment has been acquired by institutions and businesses to better use the imagery. Alternatively, LIDAR is a much newer technology and relies heavily on powerful computers and GIS software. Fortunately, both computers and GIS software



are becoming standards in geology, but there is still a certain learning curve with any new technique. Therefore, aerial photographs have the advantage of having a long history in the geologic community.

### *Required technology*

The technology required for using aerial photographs to identify landslides is relatively simple. After the photographs have been acquired, they are ready for immediate use. Given some training, a person can look at two photos side by side and see a single in-stereo image with no assistance. For high-powered magnification, an expensive stereoscope is required.

On the other hand, using LIDAR is a digital process that cannot begin without a computer and GIS software. Also, the data requires some manipulation before it can be used. In this study, several grids of data had to be merged, reprojected, shaded, and contoured before they were ready for use. However, with good instructions, these processes are not difficult. Also, if LIDAR becomes more mainstream, it is very possible that a finished product could be given to people before they begin their work, so that the preparatory time would be cut to almost nothing.

After landslides have been identified, both LIDAR imagery and aerial photographs require powerful computers and GIS software to transfer mapped geomorphic features into the digital environment.

### *Availability of data*

As previously mentioned, aerial photographs are flown regularly across the State of Washington. This photo inventory is stored at the DNR building in Olympia and the photographs are readily available. Conversely, LIDAR is only available in the Puget Lowland, though there are plans to extend the LIDAR coverage (Figure 23).

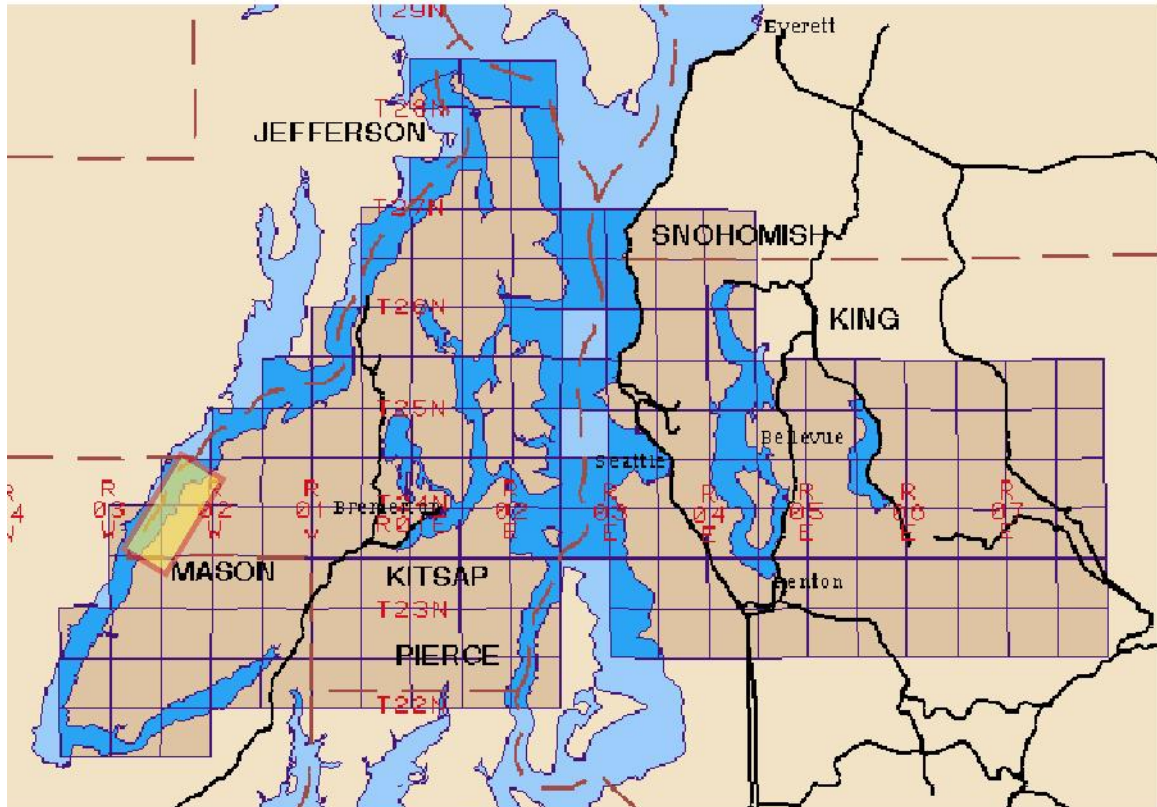


**Figure 23:** Availability of LIDAR data in Puget Lowland indicated by brown unit cells (PSLC, 2000).

### *Cost of imagery*

The DNR reports that black and white aerial photographs, like those used in this study, cost approximately \$6/kilometer<sup>2</sup> to acquire (T. J. Curtis, oral communication, 2003). They are sold for \$10 per photograph to the general public. The process used to create the orthophotographs is separate from aerial photographs. In the case of the OL-94

orthophotographs used for this project, the acquisition and ortho-rectification of the images cost \$1000 per township. For the general public, an orthophotograph covering a single township may be purchased from the DNR for \$100.

One drawback to LIDAR is its high cost. The PSLC reports that the contracted imagery costs roughly \$193/kilometer<sup>2</sup> (J. Harless, written communication, 2003).

TerraPoint LLC provides the PSLC is provided with three products: all-return data, classified bare-earth returns, and a bare-earth surface model (for this study, the classified bare-earth returns were used). Despite its high acquisition cost, the LIDAR imagery maintained by the PSLC is public domain and therefore free of charge.

### **Characterization of Sliding in Study Area**

The data collected in this thesis supports the general characterization of landslide types and mechanisms for the Hood Canal region as reported by Gryta (1975). Sliding appears to be activated during years of above average rainfall. Furthermore, this study supports the observation that stratigraphic relationships also play an important roll in controlling the spatial location of landsliding.

#### *Stratigraphic control on landsliding*

The field area studied has a variety of different types of slides occurring on steep slopes. In the southern reaches of the field area, sliding tends to be mostly shallow and colluvial, whereas farther north, deep-seated landslide complexes and shallow, colluvial slides coexist (Figure 1b). The change in the type of sliding can be correlated to changes in local stratigraphy.

In the southern portion of the field area, the stratigraphy is characterized by a veneer of till (Qgt) which overlies outwash (Qgas). Below these units is a 100-meter thick unit of pre-Vashon gravels (Qpg<sub>o</sub>) (Figure 4). This unit is composed of compact, well-rounded gravels and coarse sands with lenses of silt and clay. It persists to the shoreline.

The lower unit (Qpg<sub>o</sub>) has similar permeability and cohesive strength throughout. The homogenous and dense nature of this unit prevents water from reducing the shear strength. Without a reduction in shear strength, large deep-seated landslides do not occur. Instead, no doubt due to the steep local topography, the upper mantle of colluvium and soil moves downslope in small, localized, shallow slides. In this area, all of the 18 mapped slides were shallow (Table 5).

One half-kilometer south of Holly, the stratigraphy changes. A highly compact gray unit of stratified silts, sands, and clays with dark pieces of compressed peaty wood forms a 1-meter-high cliff at the beach (Qps). This assumed non-glacial unit is exposed for approximately 3-to-5-meters before disappearing beneath modern beach deposits. Above this unit is the previously mentioned oxidized gravels (Qpg<sub>o</sub>) and overlying the gravels is outwash (Qgas) (Figure 4).

The non-glacial unit has different properties than the overlying gravels; most importantly, the unit is an aquatard. Water pools at the interface between the non-glacial unit and the overlying gravels and increases pore pressure. During periods of high precipitation, this can result in large, deep-seated slide complexes. These slide complexes overall appear to have deep failure surfaces with many smaller, shallower slides within their boundaries. Where these large slide complexes do not exist, smaller,

shallow slides still occur on steep slopes. The non-glacial beds continue to make up the basal unit to just south of Hood Point (the northern boundary of the field area). Of the four mapped slides in this area, three were shallow and one was deep-seated (Table 5).

Near the town of Holly, the gravels (Qpg<sub>o</sub>) pinch out and are replaced by the stratigraphically overlying Vashon advance outwash (Qgas) and Vashon till (Qgt) (Figure 4). The non-glacial unit continues to act as an aquatard, which increases pore pressure at the contact between it and the overlying Vashon advance outwash sands. The local stratigraphy in this area is especially conducive to creating large landslide complexes because of the highly permeable nature of the advance outwash. The result of the permeability difference is a suite of impressive landslides. In this area, 61 slides were mapped: 19 were shallow and 42 were deep-seated (Table 5).

Deep-seated slides dominate to just south of Hood Point, where the non-glacial beds disappear. At this point the stratigraphy consists of Vashon advance outwash (Qgas) overlain by Vashon till (Qgt) (Figure 4). The result is a group of smaller, shallower slides as in the southern field area. Of the three slides mapped in this area, all were shallow (Table 5).

### **Landslide Inventory**

Plate 1 shows a complete landslide inventory created from a combination of the interpretation of aerial photographs, LIDAR imagery, and field verification.

Accompanying each slide is an ID number colored red for deep seated slides and blue for shallow landslides.

## CONCLUSION

Landslides pose a serious threat to coastal bluffs throughout the Puget Lowland, Washington and cause millions of dollars in damage each year. Accurate and precise landslide inventories can aid in minimizing future damages. Since extensive ground mapping is expensive and labor intensive, geologists rely on remote sensing techniques and limited fieldwork to create landslide inventories. Focusing on an eight-kilometer stretch of coast along Hood Canal in Kitsap County, Washington, aerial photographs, a standard in this industry, and LIDAR, a more recent technology, were compared to see which tool provides geologists with a better medium to locate and define the boundaries of landslides. The results are mixed.

Photogrammetry is effective for locating small, shallow slides occurring along coastal bluffs as well as larger, deep-seated slides, costs only \$25/mi<sup>2</sup> to fly over large photo project areas (county-wide scale), works well when vegetation cues indicate recent sliding, and is available throughout Washington State in multi-year intervals. However, photogrammetric interpretation often fails in precisely defining slide boundaries in forested terrain, is not manipulatable with respect to shadows and vertical exaggeration, and is less efficient in the field and office than LIDAR imagery. LIDAR imagery is highly effective for precisely defining landslide boundaries where the laser return from the ground is good, is efficient in the field and office, is easier to interpret than aerial photographs, and is highly manipulatable with respect to shadows and vertical exaggeration. However, LIDAR imagery does not always show smaller, shallower slide features, lacks vegetation cues, costs about \$500/ mi<sup>2</sup> to fly, and has limited availability in Washington State. Results from this comparison suggest that both methods have

strengths and weaknesses with regard to generating landslide inventories. When possible, the best approach is to use both methods in a complementary fashion.

In addition to comparing the two forms of imagery, a detailed geologic map of the Pleistocene glacial and interglacial units was created. Stratigraphy was found to control landsliding along the eastern shore of Hood Canal in the southern portion of Kitsap County. In the southern reaches of the field area, over-consolidated and impermeable units form steep slopes with small, colluvial landslides. Farther north, the basal unit is a non-glacial silty, clayey unit that acts as an aquatard below overlying sand and gravels. This interface increases pore pressure and leads to large-scale, deep-seated landslides.

## ACKNOWLEDGMENTS

I could not have completed this thesis without help from the following people: Karl Wegmann, Geologist, Department of Natural Resources, Division of Geology and Earth Resources; Steve Palmer, Geologist, Department of Natural Resources, Division of Geology and Earth Resources; Patrick Spencer, faculty advisor, Whitman College; Robert Carson, faculty advisor, Whitman College. Thanks also goes to the Whitman College Parents' Council for providing funding, the Department of Natural Resources and the Division of Geology and Earth Resources for supporting my research, the Puget Sound LIDAR Consortium for providing the LIDAR data, and Whitman College for providing resources to compose this thesis.



## APPENDIX

### Appendix 1: Landslide inventory:

Inventory ID: Final landslide inventory number that corresponds to Plate 1.

Method of location: Aerial photographs (A), LIDAR imagery (L), and in the field (F).

Probabability: Definite (Def) and probable (Prob).

Activity\_Type: State of activity as active (Act), young (Yng), or mature (Mat) and type.

Corresponding ID: ID number from aerial photographs (A), LIDAR (L), or field (none)

| ID # | Method of Identification | Probability | Activity_Type |
|------|--------------------------|-------------|---------------|
| 1    | L,F                      | Def         | Act_Shallow   |
| 2    | A,F                      | Def         | Act_Shallow   |
| 3    | A,F                      | Def         | Act_Shallow   |
| 4    | A,F                      | Def         | Act_Shallow   |
| 5    | A,F                      | Prob+       | Act_Shallow   |
| 6    | A,F                      | Prob+       | Act_Shallow   |
| 7    | F,A                      | Prob+       | Act_Shallow   |
| 8    | A                        | Prob        | Act_Shallow   |
| 9    | A,L                      | Def         | Act_Shallow   |
| 10   | A,L                      | Def         | Act_Shallow   |
| 11   | A,L,F                    | Def-        | Yng_Deep      |
| 12   | F                        | Prob        | Yng_Deep      |
| 13   | A,L,F                    | Prob        | Mat_Deep      |
| 14   | A,L,F                    | Def         | Yng_Deep      |
| 15   | A,L,F                    | Def         | Mat_Deep      |
| 16   | A,L,F                    | Def         | Act_Deep      |
| 17   | A,L,F                    | Prob+       | Yng_Deep      |
| 18   | L                        | Prob+       | Yng_Deep      |
| 19   | L,F                      | Def         | Yng_Shallow   |
| 20   | L,F                      | Def         | Act_Deep      |
| 21   | L,F                      | Def         | Act_Deep      |
| 22   | A,L,F                    | Def         | Mat_Deep      |
| 23   | A,L,F                    | Def         | Mat_Deep      |
| 24   | A,L,F                    | Def         | Act_Deep      |
| 25   | L,F                      | Def         | Act_Deep      |
| 26   | A,L,F                    | Def         | Act_Deep      |
| 27   | L,F                      | Def         | Act_Deep      |
| 28   | A,L,F                    | Def         | Act_Deep      |
| 29   | A,L,F                    | Def         | Act_Deep      |
| 30   | A,L,F                    | Def         | Mat_Shallow   |
| 31   | A,L,F                    | Def         | Act_Deep      |
| 32   | L,F                      | Prob        | Mat_Deep      |
| 33   | A,L,F                    | Def         | Act_Deep      |
| 34   | A,L,F                    | Def         | Act_Shallow   |
| 35   | A,L,F                    | Def         | Act_Deep      |
| 36   | A,L,F                    | Prob+       | Act_Shallow   |
| 37   | A,L,F                    | Prob        | Mat_Deep      |
| 38   | A,L,F                    | Prob        | Mat_Deep      |

|    |       |       |             |
|----|-------|-------|-------------|
| 39 | A,L,F | Def   | Act_Deep    |
| 40 | L     | Prob  | Mat_Deep    |
| 41 | A,L,F | Prob+ | Yng_Shallow |
| 42 | L,F   | Prob+ | Act_Shallow |
| 43 | A,L,F | Def   | Act_Shallow |
| 44 | L,F   | Prob+ | Act_Shallow |
| 45 | A,F   | Def   | Act_Shallow |
| 46 | A,F   | Prob+ | Yng_Deep    |
| 47 | A,F   | Def   | Mat_Deep    |
| 48 | A     | Def   | Act_Shallow |
| 49 | A,F   | Def   | Act_Shallow |
| 50 | A,F   | Def   | Act_Shallow |
| 51 | A,F   | Def   | Mat_Deep    |
| 52 | A,L,F | Def   | Act_Deep    |
| 53 | A,F   | Def,  | Act_Shallow |
| 54 | A,F   | Prob+ | Act_Shallow |
| 55 | A,F   | Def   | Act_Shallow |
| 56 | A,F   | Prob+ | Act_Shallow |
| 57 | A,F   | Prob+ | Act_Shallow |
| 58 | L     | Prob  | Act_Shallow |
| 59 | A,F   | Def   | Act_Shallow |
| 60 | L,F   | Prob+ | Act_Shallow |
| 61 | A,F   | Def+  | Act_Deep    |
| 62 | L,F   | Prob  | Mat_Deep    |
| 63 | A,F   | Def   | Act_Deep    |
| 64 | F     | Def   | Yng_Shallow |
| 65 | A,L,F | Prob  | Mat_Deep    |
| 66 | F     | Def   | Act_Shallow |
| 67 | L,F   | Def   | Yng_Shallow |
| 68 | F     | Prob+ | Yng_Deep    |
| 69 | A,F   | Prob  | Yng_Shallow |
| 70 | F     | Def   | Yng_Deep    |
| 71 | F     | Prob+ | Yng_Shallow |
| 72 | L,F   | Def   | Mat_Deep    |
| 73 | L     | Prob+ | Mat_Deep    |
| 74 | A,L   | Def-  | Yng_Deep    |
| 75 | A,L   | Def-  | Yng_Deep    |
| 76 | F     | Def   | Act_Deep    |
| 77 | A,L   | Prob  | Act_Shallow |
| 78 | A,F   | Def   | Act_Shallow |
| 79 | A,F   | Def   | Act_Shallow |
| 80 | F     | Def   | Act_Shallow |
| 81 | A,L   | Prob  | Mat_Deep    |
| 82 | F     | Def   | Act_Deep    |
| 83 | F     | Def   | Act_Shallow |
| 84 | A,L   | Prob  | Mat_Deep    |
| 85 | A,L   | Prob  | Mat_Deep    |
| 86 | A,F   | Def   | Act_Deep    |

## WORKS CITED

- Cruden, D. M., and D. J. Varnes, 1996, Landslide types and processes, *in* A. K. Turner and R. L. Schuster, eds., *Landslides: Investigation and mitigation: Transportation Research Board, National Research Council, Special Report 247*. Washington, D.C.: National Academy Press. p. 36-75.
- Borden, R. K., and K.G. Troost, 2001, Late Pleistocene stratigraphy in the south-central Puget Lowland, Pierce County, Washington: Washington Division of Geology and Earth Resources Report of Investigations 33, 33 p.
- Brandon, M. T., M. K. Roden-Tice, and J. I. Garver, 1998, Late Cenozoic exhumation of the Cascadia accretionary wedge in the Olympic Mountains, northwest Washington State: Geological Society of America Bulletin, v. 110, no. 8, p. 985-1009.
- Deeter, J.D., 1979, Quaternary geology and stratigraphy of Kitsap County, Washington: Masters Thesis, Western Washington University, 175 p.
- Geologic Hazards, 1998, United States Geological Survey, [accessed April 22, 2003 at [http://geohazards.cr.usgs.gov/html\\_files/landslides/about\\_ls.html](http://geohazards.cr.usgs.gov/html_files/landslides/about_ls.html)].
- Gerstel, W. J., 1997, Progress report on the geologic mapping and landslide inventory of the west-central portion of the Olympic Peninsula, Washington: Washington Geology 25, no. 4, p. 30-32.
- Greely, R., K. Bender, and R. Pappalardo, 1998, Activities in planetary geology for the physical and earth sciences: National Aeronautics and Space Administration, Educational Product, Exercise 3 [accessed April 22, 2003 at <http://teacherlink.ed.usu.edu/tlnasa/units/PlanetaryGeology/5.pdf>].
- Gryta, J. J., 1975, Landslides along the western shore of Hood Canal, Northern Mason County, Washington: Masters Thesis, North Carolina State University, 78 p.
- Haugerud, R. A., Harding, D. J., 2001, Some algorithms for virtual deforestation (VDF) of lidar topographic survey data: International Archives of Photogrammetry and Remote Sensing: v. 34, part 3/W4, Commission III, p. 211-217 [Accessed May 16, 2002 at <http://duff.geology.washington.edu/data/raster/lidar/vdf4.pdf>].
- Hofmeister, R. J., 2000, Slope failures in Oregon; GIS inventory for three 1996/97 storm events: Special Paper - Oregon, Department of Geology and Mineral Industries 34, Portland, OR, Oregon Department of Geology and Mineral Industries, United States.
- Jackson, Julia A., editor, 1997, Glossary of geology; 4th ed.: American Geological Institute, p.769.

Kockelman, W. J., 1996, Some techniques for reducing landslide hazards: Bulletin of the Association of Engineering Geologists 23, no. 1, p. 29-52.

Puget Sound LIDAR Consortium, 2002, About LIDAR, [accessed April 22, 2003 at [http://duff.geology.washington.edu/data/raster/lidar/About\\_LIDAR.htm](http://duff.geology.washington.edu/data/raster/lidar/About_LIDAR.htm)].

Ray, R. G., 1960, Aerial photographs in geologic interpretation and mapping: Geological Survey Professional Paper 373, United States Government Printing Office, Washington, 230 p.

Shipman, H., 2001, Coastal landsliding on Puget Sound: A review of landslides occurring between 1996 and 1999, Publication #01-06-019, Shorelands and Environmental Assistance Program, Washington Department of Ecology, Olympia, 87 p.

University of Washington, 2003, Glacial periods [accessed April 29, 2003 at [http://depts.washington.edu/geology/seatac\\_ice\\_limit.html](http://depts.washington.edu/geology/seatac_ice_limit.html)].

Washington Department of Ecology, 1979, Coastal zone atlas of Washington; volume 10, Kitsap County: Washington Department of Ecology, maps, scale 1:24,000.

Wegmann, K. W., and T. J. Walsh, Landslide hazard mapping in Cowlitz County--A progress report: Washington Geology, v. 29, no. 1/2, p. 30-33.

Wegmann, K. W., in press, Digital landslide inventory of the Cowlitz County Urban Corridor – Kelso to Woodland (Coweeman River to Lewis River), Cowlitz County, Washington: Washington Division of Geology and Earth Resources Report of Investigations 34.

Wieczorek, G. F., 1996, Landslide triggering mechanisms, *in* K.A. Turner and R. L. Schuster, eds., Landslides: Investigation and mitigation: Washington, D.C., National Academy Press, Transportation Research Board, National Research Council, Special Report 247, p. 12-35.